# GePUP-ES: High-order Energy-stable Projection Methods for the Incompressible Navier-Stokes Equations with No-slip Conditions

Yang Li<sup>1†</sup>, Xu Wu<sup>2,3</sup>, Jiatu Yan<sup>1</sup>, Jiang Yang<sup>3,4</sup>, Qinghai Zhang<sup>1,5,6\*</sup>, Shubo Zhao<sup>5†</sup>

- <sup>1</sup> School of Mathematical Sciences, Zhejiang University, Hangzhou, 310058, Zhejiang, China.
- <sup>2</sup> Department of Applied Mathematics, The Hong Kong Polytechnic University, Kowloon, 100872, Hong Kong, China.
- <sup>3</sup> SUSTech International Center for Mathematics, Southern University of Science and Technology, Shenzhen, 518055, Guangdong, China.
- <sup>4</sup> National Center for Applied Mathematics Shenzhen (NCAMS), Southern University of Science and Technology, Shenzhen, 518055, Guangdong, China.
- <sup>5</sup> College of Mathematics and System Sciences, Xinjiang University, Urumqi, 830046, Xinjiang, China.
  - <sup>6</sup> Shanghai Institute for Advanced Study of Zhejiang University, Shanghai AI Laboratory, Shanghai, 200000, China.

\*Corresponding author(s). E-mail(s): qinghai@zju.edu.cn;
Contributing authors: 3150104952@zju.edu.cn;
11849596@mail.sustech.edu.cn; 12235038@zju.edu.cn;
yangj7@sustech.edu.cn; shubomath@stu.xju.edu.cn;
†These authors contributed equally to this work and should be considered as co-first authors.

### Abstract

Inspired by the unconstrained PPE (UPPE) formulation [Liu, Liu, & Pego 2007 Comm. Pure Appl. Math., 60 pp. 1443], we previously proposed the GePUP formulation [Zhang 2016 J. Sci. Comput., 67 pp. 1134] for numerically solving the incompressible Navier-Stokes equations (INSE) on no-slip domains. In this

paper, we propose GePUP-E and GePUP-ES, variants of GePUP that feature (a) electric boundary conditions with no explicit enforcement of the no-penetration condition, (b) equivalence to the no-slip INSE, (c) exponential decay of the divergence of an initially non-solenoidal velocity, and (d) monotonic decrease of the kinetic energy. Different from UPPE, the GePUP-E and GePUP-ES formulations are of strong forms and are designed for finite volume/difference methods under the framework of method of lines. Furthermore, we develop semi-discrete algorithms that preserve (c) and (d) and fully discrete algorithms that are fourthorder accurate for velocity both in time and in space. These algorithms employ algebraically stable time integrators in a black-box manner and only consist of solving a sequence of linear equations in each time step. Results of numerical tests confirm our analysis.

Keywords: Incompressible Navier-Stokes equations with no-slip conditions, Fourth-order accuracy, Projection methods, GePUP, Energy stability, Scalar auxiliary variable

MSC Classification: Primary 76D05, 65M20

# 1 Introduction

The incompressible Navier-Stokes equations (INSE) with no-slip conditions read

$$\frac{\partial \mathbf{u}}{\partial t} + \mathbf{u} \cdot \nabla \mathbf{u} = \mathbf{g} - \nabla p + \nu \Delta \mathbf{u} \quad \text{in } \Omega,$$

$$\nabla \cdot \mathbf{u} = 0 \quad \text{in } \Omega,$$
(1a)

$$\nabla \cdot \mathbf{u} = 0 \qquad \text{in } \Omega, \tag{1b}$$

$$\mathbf{u} = \mathbf{0}$$
 on  $\partial \Omega$ , (1c)

where  $t \in [0, +\infty)$  is time,  $\Omega$  a domain, i.e., a bounded connected open subset of  $\mathbb{R}^D$ ,  $\partial\Omega$  the domain boundary, **g** the external force, p the pressure, **u** the velocity, and  $\nu$ the kinematic viscosity.

The INSE in (1) govern an enormous range of real-world phenomena such as blood flow, turbulence, atmosphere and ocean currents. As a fundamental and notoriously difficult problem, the well-posedness of the INSE (in  $\mathbb{R}^3$  and  $\mathbb{R}^3/\mathbb{Z}^3$  [1]) is selected by Smale [2] on his list of 18 math problems for the 21st century and by the Clay Institute on the list of 7 millennium problems [3]. Therefore, numerical computation appears to be the only viable way for now to obtain approximate solutions of the INSE. On the other hand, numerical computation may help the analytic understanding of INSE. As an example, Li [4] has recently shown that a bounded numerical solution with a small mesh size implies the existence of a smooth solution to the INSE.

#### 1.1 Challenges for the design of numerical solvers

The aim of numerically solving differential equations is to efficiently, accurately, and faithfully reproduce the physical processes modeled by the equations. Specific to numerically solving the INSE are four major challenges that we confront in this work.

- 1. How to fulfill the solenoidal condition (1b) and other physical constraints such as the monotonic decrease of the kinetic energy?
- 2. How to ensure various types of numerical stability?
- 3. How to obtain high-order convergence both in time and in space?
- 4. How to decouple time integration from spatial discretization so that (i) the entire solver is constituted by orthogonal modules for these aspects, and (ii) solution methods for each aspect can be employed in a black-box manner and thus easily changed to make the entire INSE solver versatile?
- (A) concerns the prominent feature of mass conservation: neither source nor sink exists anywhere inside the domain. It is well-known that a violation of (1b), even with small errors, might lead to qualitatively different flow patterns, especially for large Reynolds numbers. Another important physical constraint to be fulfilled in this work is the monotonic decrease of the total kinetic energy as defined in (51).
- In (B), a crucial and indispensable type of numerical stability is the eigenvalue stability for the main evolutionary variable, which is typically the velocity. In addition, preserving the monotonicity of kinetic energy is equivalent to ensuring numerical stability on the velocity with respect to the 2-norm.

Challenge (C) concerns accuracy and efficiency. Near no-slip boundaries, flows at high Reynolds numbers tend to develop structures of multiple length scales and time scales. A numerical method should resolve all scales that are relevant to the important physics. Compared with fourth- and higher-order methods, first- and second-order methods have simpler algorithms and cheaper computations, but towards a given accuracy the computational resources may be rapidly exhausted. It is shown both theoretically and numerically in [5, Sec. 7] that fourth-order methods may have a large efficiency advantage over second-order methods.

Challenge (C) also concerns faithfully simulating flows where velocity derivatives such as vorticity crucially affect the physics. For first-order finite volume/difference methods, the computed velocity converges, but the vorticity does not, nor does the velocity gradient tensor. Consequently, the O(1) error in  $\nabla \mathbf{u}$  may lead to structures different from that of the original flow. In other words, it is not clear whether or not solutions of a first-order method have converged to the *right* physics. Similar suspicions apply to second-order methods for flows where second derivatives of the velocity are important.

Challenge (D) concerns versatility and user-friendliness of the numerical solver. To cater for the problem at hand, it is often desirable to change the time integrator from one to another. For example, flows with high viscosity are usually stiff while those with small viscosity are not; accordingly, an implicit time integrator should be used in the former case while an explicit one is usually suitable for the latter. If the internal details of a time integrator are coupled into the INSE solver in a boilerplate manner, it would be difficult and very inconvenient to change the time integrator; see also the discussion in the paragraph under (4). Hence a time integrator should be treated as a black box: for the ordinary differential equation (ODE)  $\frac{\mathrm{d}U}{\mathrm{d}t} = f(U,t)$ , we should only need to feed into the time integrator the initial condition  $U^n$  and samples of f at a number of time instances to get the solution  $U^{n+1}$  from the black box.

This versatility further leads to user-friendliness. Analogous to orthogonal bases of a vector space, the mutually independent policies span a space of solvers, where each solver can be conveniently assembled by selecting a module for each constituting policy. For example, a specific INSE solver is formed by choosing semi-implicit Runge-Kutta (RK) for time integration, finite volume for spatial discretization, fourth-order for accuracy and so on; see Table 1.

# 1.2 Some previous methods

In the original projection method independently proposed by Chorin [6] and Temam [7], the initial condition  $\mathbf{u}^n \approx \mathbf{u}(t^n)$  is first advanced to an auxiliary velocity  $\mathbf{u}^*$ without worrying about the pressure gradient term and then  $\mathbf{u}^*$  is projected to the divergence-free space to obtain  $\mathbf{u}^{n+1}$ ,

$$\frac{\mathbf{u}^* - \mathbf{u}^n}{k} = -\mathbf{C}(\mathbf{u}^*, \mathbf{u}^n) + \mathbf{g}^n + \nu \mathbf{L} \mathbf{u}^*,$$

$$\mathbf{u}^{n+1} = \mathbf{P} \mathbf{u}^*,$$
(2a)

$$\mathbf{u}^{n+1} = \mathbf{P}\mathbf{u}^*,\tag{2b}$$

where k is the time step size,  $t^n$  is the starting time of the nth step,  $\mathbf{g}^n \approx \mathbf{g}(t^n)$ ,  $\mathbf{C}(\mathbf{u}^*, \mathbf{u}^n) \approx [(\mathbf{u} \cdot \nabla)\mathbf{u}](t^n)$ , and **L** and **P** are discrete approximations of the Laplacian  $\Delta$  and the Leray-Helmholtz projection  $\mathcal{P}$ , respectively; see Section 2.1.

# 1.2.1 Second-order methods with fractional time stepping

Chorin and Temam's original projection method is first-order accurate and its improvement to the second order has been the aim of many subsequent works; see, e.g., [8–13] and references therein. A common basis of many second-order methods is the temporal discretization of (1) with the trapezoidal rule,

$$\frac{\mathbf{u}^{n+1} - \mathbf{u}^n}{k} + \nabla p^{n+\frac{1}{2}} = -[(\mathbf{u} \cdot \nabla)\mathbf{u}]^{n+\frac{1}{2}} + \mathbf{g}^{n+\frac{1}{2}} + \frac{\nu}{2}\Delta(\mathbf{u}^{n+1} + \mathbf{u}^n), \quad (3a)$$

$$\nabla \cdot \mathbf{u}^{n+1} = 0, \tag{3b}$$

where  $p^{n+\frac{1}{2}} \approx p(t^{n+\frac{1}{2}})$ ,  $\mathbf{g}^{n+\frac{1}{2}} \approx \mathbf{g}(t^{n+\frac{1}{2}})$ , and  $[(\mathbf{u} \cdot \nabla)\mathbf{u}]^{n+\frac{1}{2}} \approx [(\mathbf{u} \cdot \nabla)\mathbf{u}](t^{n+\frac{1}{2}})$  are numerical approximations at the mid-time  $t^{n+\frac{1}{2}} = \frac{1}{2}(t^n + t^{n+1})$  of the nth step.

Replacing the gradient  $\nabla$ , the divergence  $\nabla$ , and the Laplacian  $\Delta$  in (3) with their second-order discrete counterparts G, D, and L, respectively, we have

$$A \begin{bmatrix} \mathbf{u}^{n+1} \\ p^{n+\frac{1}{2}} \end{bmatrix} := \begin{bmatrix} \frac{1}{k} \mathbf{I} - \frac{\nu}{2} \mathbf{L} & \mathbf{G} \\ -\mathbf{D} & \mathbf{0} \end{bmatrix} \begin{bmatrix} \mathbf{u}^{n+1} \\ p^{n+\frac{1}{2}} \end{bmatrix} = \mathbf{F}.$$
 (4)

Since  $\mathbf{G}^T = -\mathbf{D}$ , the matrix A has a saddle point structure and the above method is often called the saddle point approach. Despite its simplicity, this approach has two main disadvantages. First, the spatial discretization and time integration are coupled in a boilerplate manner and thus a change of either part would demand a complete rederivation of the matrix A. For fourth- or higher-order accuracy in time integration,

it is often too complicated to have an explicit expression of the matrix A, as A contains all internal details of the time integrator. Consequently, it is highly difficult for this approach to address challenges (C) and (D). Second, it is challenging [14] to efficiently solve the linear system (4) since all the velocity components and the pressure are coupled into a big unknown vector; in contrast, Chorin's projection method only requires the solutions of linear systems with the unknowns as either the pressure or a velocity component.

Following (3), many second-order projection methods with fractional stepping can be united [13] as follows,

• choose a boundary condition  $B(u^*) = 0$  to solve for  $u^*$ ,

$$\frac{\mathbf{u}^* - \mathbf{u}^n}{k} + \nabla q = -[(\mathbf{u} \cdot \nabla)\mathbf{u}]^{n + \frac{1}{2}} + \mathbf{g}^{n + \frac{1}{2}} + \frac{\nu}{2}\Delta(\mathbf{u}^* + \mathbf{u}^n); \tag{5}$$

• enforce (3b) with a discrete projection so that

$$\mathbf{u}^* = \mathbf{u}^{n+1} + k\nabla\phi^{n+1},\tag{6}$$

• update the pressure by

$$p^{n+\frac{1}{2}} = q + \mathbf{U}(\phi^{n+1}),\tag{7}$$

where the specific forms of q,  $\mathbf{B}(\mathbf{u}^*)$ , and  $\mathbf{U}(\phi^{n+1})$  vary from one method to another. For examples, the method of Bell, Colella & Glaz (BCG) [9] is specified by

$$q = p^{n - \frac{1}{2}}, \quad \mathbf{B}(\mathbf{u}^*) = \mathbf{u}^*|_{\partial\Omega} = \mathbf{0}, \quad \nabla p^{n + \frac{1}{2}} = \nabla p^{n - \frac{1}{2}} + \nabla \phi^{n+1},$$
 (8)

while that of Kim & Moin [8] by

$$q = 0, \quad \mathbf{n} \cdot \mathbf{u}^*|_{\partial\Omega} = 0, \quad \boldsymbol{\tau} \cdot \mathbf{u}^*|_{\partial\Omega} = k\boldsymbol{\tau} \cdot \nabla \phi^n|_{\partial\Omega},$$
 (9a)

$$\nabla p^{n+\frac{1}{2}} = \nabla \phi^{n+1} - \frac{\nu k}{2} \nabla \Delta \phi^{n+1}. \tag{9b}$$

As observed by Brown, Cortez & Minion [13], the choices of q,  $\mathbf{B}(\mathbf{u}^*)$ , and  $\mathbf{U}(\phi^{n+1})$  are not independent. Indeed, substitute (6) into (5), subtract (3a), and we have

$$\nabla p^{n+\frac{1}{2}} = \nabla q + \nabla \phi^{n+1} - \frac{\nu k}{2} \Delta \nabla \phi^{n+1}. \tag{10}$$

Consequently, the pressure computed by (8) is only first-order accurate [13] because its pressure update formula is at an O(k) discrepancy with (10). On the other hand, the pressure update formula (9b) complies with (10) due to the commutativity of Laplacian and the gradient, but (9b) and (6) imply  $p^{n+\frac{1}{2}} = \phi^{n+1} - \frac{\nu}{2} \nabla \cdot \mathbf{u}^*$ , which may deteriorate the pressure accuracy to the first order [13]. Nonetheless, both methods (8) and (9) are second-order accurate for the velocity.

Fractional-stepping methods have been successful, but it is difficult to improve them to fourth- and higher-order accuracy. As discussed above, the choices of q,

 $\mathbf{B}(\mathbf{u}^*)$ , and  $\mathbf{U}(\phi^{n+1})$  are coupled according to internal details of the time integrator. Consequently, switching from one time integrator to another calls for a new derivation. Furthermore, although appearing divorced, the velocity and the pressure are still implicitly coupled by the boundary condition of the auxiliary variable  $\mathbf{u}^*$ , with the coupling determined not by physics but still by internal details of the time integrator. Therefore, the approach of fractional-stepping methods is not suitable for tackling challenges (C) and (D).

#### 1.2.2 The formulation of the pressure Poisson equation (PPE)

As a specialization of Newton's second law, the momentum equation (1a) can be rewritten as

$$\mathbf{a}^* = \mathbf{a} + \nabla p,\tag{11}$$

where the Eulerian accelerations are vector functions

$$\mathbf{a} := \frac{\partial \mathbf{u}}{\partial t}, \quad \mathbf{a}^* := -\mathbf{u} \cdot \nabla \mathbf{u} + \mathbf{g} + \nu \Delta \mathbf{u}.$$
 (12)

The PPE describes an *instantaneous* relation between the pressure and the velocity in the INSE and, on no-slip domains, has the form

$$\Delta p = \nabla \cdot (\mathbf{g} - \mathbf{u} \cdot \nabla \mathbf{u} + \nu \Delta \mathbf{u}) \quad \text{in } \Omega, \tag{13a}$$

$$\mathbf{n} \cdot \nabla p = \mathbf{n} \cdot (\mathbf{g} + \nu \Delta \mathbf{u}) \qquad \text{on } \partial \Omega, \tag{13b}$$

where (13b) follows from the normal component of (1a) and the no-slip conditions (1c) while (13a) from the divergence of (1a) and the divergence-free condition (1b). For the PPE with other boundary conditions, (13b) should be replaced with the normal component of (11). As explained in Section 2.1, the pressure gradient is uniquely determined from  $\mathbf{a}^*$  by  $\nabla p = (\mathcal{I} - \mathscr{P})\mathbf{a}^*$  where  $\mathcal{I}$  and  $\mathscr{P}$  are the identity operator and the Leray-Helmholtz projection, respectively. Thus neither the initial condition nor the boundary condition of the pressure p is needed in the INSE.

(1a), (1c), (13), and the additional boundary condition  $\nabla \cdot \mathbf{u} = 0$  on  $\partial \Omega$  are collectively called the PPE formulation of the INSE on no-slip domains [15]. In terms of computation, however, the PPE formulation has a decisive advantage over the original INSE. If (1a) is discretized in time with (1b) as a constraint, the resulting index-2 differential algebraic system may suffer from large order reductions [16]. In contrast, replacing the divergence-free constraint with the PPE avoids this difficulty. As such, the PPE formulation allows the time integrator to be treated as a black box and thus to be easily changed; indeed, the pressure is an implicit function of  $\mathbf{u}$  and its interaction with  $\mathbf{u}$  is completely decoupled from internal details of the time integrator. Also, there is no need to introduce nonphysical auxiliary variables. These advantages of the PPE formulation lead to quite a number of successful numerical methods [15, 17–22].

Unfortunately, as observed by Liu, Liu & Pego [20], (1a) and (13a) yield

$$\frac{\partial \nabla \cdot \mathbf{u}}{\partial t} = 0; \tag{14}$$

this degenerate equation implies that in the PPE formulation we have no control over  $\nabla \cdot \mathbf{u}$  and its evolution is up to the particularities of the numerical schemes. Our tests show that a fourth-order finite-volume method-of-lines (MOL) discretization of the PPE formulation is unstable, with the computed velocity divergence growing indefinitely near the domain boundary.

#### 1.2.3 The formulation of unconstrained PPE (UPPE)

By applying the Leray-Helmholtz projection  $\mathcal{P}$  to (11), Liu, Liu & Pego [20] obtained

$$\frac{\partial \mathbf{u}}{\partial t} - \mathcal{P}\mathbf{a}^* = \nu \nabla (\nabla \cdot \mathbf{u}), \tag{15}$$

where the zero right-hand side (RHS) is added for stability reasons. The divergence of (15) and the second identity in (27) give

$$\frac{\partial(\nabla \cdot \mathbf{u})}{\partial t} = \nu \Delta(\nabla \cdot \mathbf{u}),\tag{16}$$

which, by the maximum principle of the heat equation, dictates an exponential decay of a nonzero  $\nabla \cdot \mathbf{u}$  in  $\Omega$ . A juxtaposition of (16) and (14) exposes a prominent advantage of (15) that any divergence residue is now well over control.

With the identity  $\nabla(\nabla \cdot \mathbf{u}) = \Delta(\mathcal{I} - \mathcal{P})\mathbf{u}$  and the Laplace-Leray commutator  $[\Delta, \mathcal{P}] := \Delta \mathcal{P} - \mathcal{P}\Delta$  (see Section 2.2), Liu, Liu & Pego [20] rewrote (15) as

$$\frac{\partial \mathbf{u}}{\partial t} + \mathcal{P}(\mathbf{u} \cdot \nabla \mathbf{u} - \mathbf{g}) + \nu [\Delta, \mathcal{P}] \mathbf{u} = \nu \Delta \mathbf{u}, \tag{17}$$

which provides a fresh viewpoint of the INSE as a controlled perturbation of the vector diffusion equation  $\frac{\partial \mathbf{u}}{\partial t} = \nu \Delta \mathbf{u}$ . For  $\mathbf{u} \in H^2 \cap H^1_0(\Omega, \mathbb{R}^D)$  with  $\mathcal{C}^3$  boundary  $\partial \Omega$ , they gave a sharp bound on  $\|[\Delta, \mathcal{P}]\mathbf{u}\|$  in terms of  $\|\Delta\mathbf{u}\|$  and proved the unconditional stability and convergence of a first-order scheme,

$$\langle \nabla p^n, \nabla \phi \rangle = \langle \mathbf{g}^n - \mathbf{u}^n \cdot \nabla \mathbf{u}^n + \nu \Delta \mathbf{u}^n - \nu \nabla \nabla \cdot \mathbf{u}^n, \nabla \phi \rangle,$$
 (18a)

$$\frac{\mathbf{u}^{n+1} - \mathbf{u}^n}{k} + \nabla p^n = \mathbf{g}^n - \mathbf{u}^n \cdot \nabla \mathbf{u}^n + \nu \Delta \mathbf{u}^{n+1} \quad \text{in } \Omega,$$
 (18b)

$$\mathbf{u}^{n+1} = \mathbf{0} \qquad \qquad \text{on } \partial\Omega, \tag{18c}$$

where (18a) is the PPE in weak form with  $\phi \in H^1(\Omega)$  and  $\langle \mathbf{u}, \mathbf{v} \rangle := \int_{\Omega} \mathbf{u} \cdot \mathbf{v} \, dV$ .

Based on their UPPE formulation, the same authors developed a slip-corrected projection method [21] that is third-order accurate both in time and in space.

So far the UPPE formulation only concerns finite element methods based on the weak formulation. It is worthwhile to adapt UPPE to a strong formulation for the MOL discretization with finite volume or finite difference methods, as this may be a viable way to answer the challenges posed in Section 1.1. From (17) and the contents

in Sections 2.2 and 2.3, a strong form of UPPE can be deduced [21] as

$$\frac{\partial \mathbf{u}}{\partial t} + \mathbf{u} \cdot \nabla \mathbf{u} = \mathbf{g} - \nabla p + \nu \Delta \mathbf{u} \qquad \text{in } \Omega, \tag{19a}$$

$$\mathbf{u} = \mathbf{0} \qquad \qquad \text{on } \partial\Omega, \tag{19b}$$

$$\Delta p = \nabla \cdot (\mathbf{g} - \mathbf{u} \cdot \nabla \mathbf{u}) \qquad \text{in } \Omega, \tag{19c}$$

$$\mathbf{n} \cdot \nabla p = \mathbf{n} \cdot (\mathbf{g} + \nu \Delta \mathbf{u} - \nu \nabla \nabla \cdot \mathbf{u}) \quad \text{on } \partial \Omega.$$
 (19d)

The PPE (13) and the UPPE (19c,d) have slightly different forms and nonetheless a crucial distinction: it follows from the divergence of (19a) that (19c) leads to (16) whereas (13a) leads to (14).

Unfortunately, (19) is not yet suitable for the design of MOL-type finite volume and finite difference methods, due to two main reasons.

- 1. The Leray-Helmholtz projection is absent in (19) and thus any projection on the velocity in an MOL algorithm would be a mismatch of the numerical algorithm to the governing equations. Of course one can replace the velocity  $\mathbf{u}$  with  $\mathscr{P}\mathbf{u}$  in (19), but which should be replaced? In other words, which  $\mathbf{u}$ 's in (19) should be projected in MOL?
- 2. It is difficult for a discrete projection **P** with fourth- and higher-order accuracy to satisfy all properties of the Leray-Helmholtz projection  $\mathscr{P}$  in (27). In particular, the discretely projected velocity may not be divergence-free. Then how does the approximation error of **P** to  $\mathscr{P}$  affect the stability of the ODE system under the MOL framework? It is neither clear nor trivial how to answer this question with (19).

# 1.2.4 The formulation of generic projection and unconstrained PPE (GePUP)

A generic projection is a linear operator  $\mathcal{P}$  on a vector space satisfying

$$\mathcal{P}\mathbf{u} = \mathbf{w} := \mathbf{u} - \nabla \phi,\tag{20}$$

where  $\phi$  is a scalar function and  $\nabla \cdot \mathbf{w} = 0$  may or may not hold. Since  $\phi$  is not specified in terms of  $\mathbf{w}$ , (20) is not a precise definition of  $\mathcal{P}$ , but rather a characterization of a family of operators, which, in particular, includes the Leray-Helmholtz projection  $\mathscr{P}$ .  $\mathscr{P}$  can be used to perturb  $\mathbf{u}$  to some non-solenoidal velocity  $\mathbf{w}$  and is thus more flexible than  $\mathscr{P}$  in characterizing discrete projections that fail to fulfill the divergence-free constraint exactly.

Inspired by Liu, Liu & Pego [20], Zhang [5] proposed the GePUP formulation of the INSE based on a commutator of the generic projection and the Laplacian. In order to accommodate the fact that the discrete velocity might not be divergence-free, the evolutionary variable of the GePUP formulation (21) is designed to be a non-solenoidal velocity  $\mathbf{w} = \mathcal{P}\mathbf{u}$  instead of the divergence-free velocity  $\mathbf{u}$  in the UPPE formulation (19). More precisely, the evolutionary variable  $\mathbf{u}$  in the time-derivative term  $\frac{\partial \mathbf{u}}{\partial t}$  is perturbed to a non-solenoidal velocity  $\mathbf{w} := \mathbf{u} - \nabla \phi$  where  $\phi$  is some scalar function;

meanwhile in the diffusion term we change  $\mathbf{u}$  to  $\mathbf{w}$  to set up a mechanism that drives the divergence towards zero. Then, there is no need to worry about the influence of  $\nabla \cdot \mathbf{w} \neq 0$  on numerical stability because the evolution of  $\mathbf{w}$  is not subject to the divergence-free constraint. These ideas lead to the GePUP formulation:

$$\frac{\partial \mathbf{w}}{\partial t} = \mathbf{g} - \mathbf{u} \cdot \nabla \mathbf{u} - \nabla q + \nu \Delta \mathbf{w} \quad \text{in } \Omega, \tag{21a}$$

$$\mathbf{w} = \mathbf{0}, \quad \mathbf{u} \cdot \boldsymbol{\tau} = 0, \quad \text{on } \partial\Omega,$$
 (21b)

$$\mathbf{u} = \mathscr{P}\mathbf{w} \qquad \qquad \text{in } \Omega, \tag{21c}$$

$$\mathbf{u} \cdot \mathbf{n} = 0 \qquad \text{on } \partial\Omega, \tag{21d}$$

$$\Delta q = \nabla \cdot (\mathbf{g} - \mathbf{u} \cdot \nabla \mathbf{u}) \qquad \text{in } \Omega, \tag{21e}$$

$$\mathbf{n} \cdot \nabla q = \mathbf{n} \cdot (\mathbf{g} + \nu \Delta \mathbf{u} - \nu \nabla \nabla \cdot \mathbf{u}) \quad \text{on } \partial \Omega.$$
 (21f)

By (21), w satisfies the heat equation

$$\frac{\partial \left(\nabla \cdot \mathbf{w}\right)}{\partial t} = \nu \Delta \left(\nabla \cdot \mathbf{w}\right) \quad \text{in } \Omega, \tag{22}$$

which, combined with  $\nabla \cdot \mathbf{w} = 0$  or  $\mathbf{n} \cdot \nabla \nabla \cdot \mathbf{w} = 0$  on  $\partial \Omega$ , drives  $\nabla \cdot \mathbf{w}$  towards zero. The GePUP formulation (21) not only retains the advantages of UPPE, but also provides certain degrees of freedom in the design of high-order projection methods.

## 1.3 The contribution of this work

In this work, we couple GePUP with the electric boundary conditions [22, 23] and the scalar auxiliary variable (SAV) approach [24, 25] to propose GePUP-E and GePUP-ES, variants of GePUP that enforce the solenoidal conditions, preserve energy stability, decouple time integration from spatial discretization, and lead to versatile algorithms that are fourth-order accurate both in time and in space. The letter 'E' in the acronyms stands for the electric boundary conditions while the letter 'S' for the SAV approach; altogether 'ES' also stands for energy stability.

GePUP-E and GePUP-ES answer all the challenges (A–D) posed in Section 1.1.

- We establish the GePUP-E formulation in (39) on solid ground by proving their equivalence to the INSE, the convergence of the non-solenoidal velocity w to the divergence-free velocity u, the exponential decay of the divergence ∇·w, and the monotonic decrease of the kinetic energy. GePUP-E resolves the difficulties in (RSN-1,2).
- 2. By coupling GePUP-E to SAV [24, 25], we propose the GePUP-ES formulation in (54), design a family of semi-discrete GePUP-ES algorithms, and prove their energy stability in Theorem 10.
- 3. Based on (CTB-2), we further propose a family of fully discrete INSE solvers, named GePUP-ES-SDIRK, to answer all challenges in (A–D).

(CTB-1,2,3) are explained in Sections 3, 4, and 5, respectively. In Section 2, we introduce notation to make this paper somewhat self-contained. We test GePUP-ES-SDIRK in Section 6 and draw conclusions in Section 7.

## 2 Preliminaries

Throughout this paper, we denote by  $\langle \cdot, \cdot \rangle$  the  $L^2$  inner product of vector- (or scalar-) valued functions  $\mathbf{u}$  and  $\mathbf{v}$  over  $\Omega$ ,  $\langle \mathbf{u}, \mathbf{v} \rangle := \int_{\Omega} \mathbf{u} \cdot \mathbf{v} \, dV$ , and by  $\| \cdot \|$  the induced  $L^2$ norm  $\|\mathbf{u}\| := \sqrt{\langle \mathbf{u}, \mathbf{u} \rangle}$ .

# 2.1 The Leray-Helmholtz projection $\mathscr{P}$

This subsection hinges on the following well-known result on boundary value problems (BVPs).

**Theorem 1** (Solvability of BVPs with pure Neumann conditions). Suppose f and g are two sufficiently smooth functions. Then there exists a unique solution (up to an additive constant) for the Neumann BVP

$$\Delta \phi = f \qquad in \ \Omega; \tag{23a}$$

$$\Delta \phi = f \qquad \text{in } \Omega; \tag{23a}$$

$$\mathbf{n} \cdot \nabla \phi = g \qquad \text{on } \partial \Omega \tag{23b}$$

if and only if  $\int_{\Omega} f \, dV = \int_{\partial \Omega} g \, dA$ .

**Theorem 2** (Helmholtz decomposition). A continuously differentiable vector field  $\mathbf{v}^*$ in a domain  $\Omega$  can be uniquely decomposed into a divergence-free part  ${f v}$  and a curl-free part  $\nabla \phi$ ,

$$\mathbf{v}^* = \mathbf{v} + \nabla \phi, \tag{24}$$

where  $\mathbf{v} \cdot \mathbf{n}$  is given a priori on  $\partial \Omega$  and satisfies  $\oint_{\partial \Omega} \mathbf{v} \cdot \mathbf{n} = 0$ .

*Proof.* The decomposition can be realized by solving

$$\begin{cases} \Delta \phi = \nabla \cdot \mathbf{v}^* & \text{in } \Omega, \\ \mathbf{n} \cdot \nabla \phi = \mathbf{n} \cdot (\mathbf{v}^* - \mathbf{v}) & \text{on } \partial \Omega, \end{cases}$$
 (25)

since Theorem 1 uniquely determines  $\nabla \phi$  with  $\oint_{\partial\Omega} \mathbf{v} \cdot \mathbf{n} = 0$ . 

The Leray-Helmholtz projection  $\mathcal{P}$  is an idempotent operator that maps a vector field  $\mathbf{v}^*$  to its divergence-free part  $\mathbf{v}$ , c.f. the decomposition (24), i.e.,

$$\mathscr{P}\mathbf{v}^* := \mathbf{v} = \mathbf{v}^* - \nabla\phi. \tag{26}$$

The proof of Theorem 2 implies the constructive form

$$\mathscr{P} = \mathcal{I} - \nabla(\Delta_n)^{-1} \nabla \cdot,$$

where  $(\Delta_n)^{-1}$  denotes solving (25). For a  $\mathcal{C}^1$  vector field  $\mathbf{v}^*$  and a  $\mathcal{C}^1$  scalar field  $\phi$ , we have

$$\mathscr{P}^2 = \mathscr{P}, \quad \nabla \cdot \mathscr{P} \mathbf{v}^* = 0, \quad \mathscr{P} \nabla \phi = \mathbf{0}.$$
 (27)

## 2.2 The Laplace-Leray commutator $\Delta \mathscr{P} - \mathscr{P} \Delta$

On periodic domains,  $\Delta$  and  $\mathscr{P}$  commute. However, one main difficulty for no-slip domains is the fact that  $\Delta \mathscr{P} - \mathscr{P}\Delta \neq \mathbf{0}$ . In this subsection we rephrase several results in [20].

Lemma 1. The divergence-gradient commutator defined as

$$\mathcal{B} = [\nabla \cdot, \nabla] := \Delta - \nabla \nabla \cdot \tag{28}$$

satisfies  $\nabla \cdot \mathcal{B} = 0$ ,  $\Delta \mathscr{P} = \mathcal{B}$ , and in three dimensions  $\mathcal{B} = -\nabla \times \nabla \times$ .

*Proof.*  $\nabla \cdot \mathcal{B} = 0$  follows from (28) and  $\Delta \nabla \cdot = \nabla \cdot \Delta$  while  $\mathcal{B}\mathbf{v}^* = -\nabla \times \nabla \times \mathbf{v}^*$  from the tensor notation and the epsilon-delta relation.  $\Delta \mathscr{P} = \mathcal{B}$  holds because

$$\Delta \mathscr{P} \mathbf{v}^* = \Delta (\mathbf{v}^* - \nabla \phi) = \Delta \mathbf{v}^* - \nabla \Delta \phi = \Delta \mathbf{v}^* - \nabla \nabla \cdot \mathbf{v}^*, \tag{29}$$

where we have applied (26), the commutativity of  $\Delta$  and  $\nabla$ , and (28).

With  $\mathscr{P}\nabla\phi = \mathbf{0}$  in (27), the first and third terms in (29) lead to

$$\mathscr{P}\Delta\mathscr{P} = \mathscr{P}\Delta\tag{30}$$

because  $\mathscr{P}\Delta\mathscr{P}\mathbf{v}^* = \mathscr{P}\Delta\mathbf{v}^*$  holds for any sufficiently smooth vector field  $\mathbf{v}^*$ .

Then Lemma 1 and (30) give

Corollary 1. The Laplace-Leray commutator is

$$[\Delta, \mathscr{P}] := \Delta \mathscr{P} - \mathscr{P} \Delta = (\mathcal{I} - \mathscr{P}) \Delta \mathscr{P} = (\mathcal{I} - \mathscr{P}) \mathcal{B} = -(\mathcal{I} - \mathscr{P}) (\nabla \times \nabla \times), \quad (31)$$

where  $\mathcal{I}$  is the identity operator and the last equality holds only in three dimensions.

#### 2.3 The Stokes pressure

By (31), the action of the Laplace-Leray commutator on any vector field  $\mathbf{v}^*$  results in the gradient of some scalar field. In the case of  $\mathbf{v}^*$  being the velocity  $\mathbf{u}$  in the INSE, the scalar is known as the *Stokes pressure* [20]:

$$\nabla p_s := (\Delta \mathscr{P} - \mathscr{P} \Delta) \mathbf{u}. \tag{32}$$

It follows from (31) and (32) that

$$\mathcal{B}\mathbf{u} = \mathscr{P}\mathcal{B}\mathbf{u} + \nabla p_s.$$

Then (27) and  $\nabla \cdot \mathcal{B} = 0$  in Lemma 1 yield  $\Delta p_s = 0$ , i.e., the Stokes pressure is harmonic. Interestingly, the vector field  $\nabla p_s$  is both divergence-free and curl-free.

Define another scalar  $p_c$  as

$$\nabla p_c := (\mathcal{I} - \mathscr{P}) \left( \mathbf{g} - \mathbf{u} \cdot \nabla \mathbf{u} \right). \tag{33}$$

Apply the Leray-Helmholtz projection to (1a), use the commutator (31), invoke the definitions (32) and (33), and we have

$$\nabla p = \nabla p_c + \nu \nabla p_s.$$

The pressure gradient in the INSE consists of two parts:  $\nabla p_c$  balances the divergence of the forcing term and the nonlinear convection term while  $\nabla p_s$  accounts for the Laplace-Leray commutator. In the two limiting cases of  $\nu \to 0$  and  $\nu \to +\infty$ , the pressure gradient is dominated by  $\nabla p_c$  and  $\nu \nabla p_s$ , respectively.

#### 2.4 Vector Identities

A proof of the following theorem can be found in a standard text on differentiable manifolds such as [27].

**Theorem 3** (Gauss-Green). A scalar or vector function  $u \in C^1(\overline{\Omega})$  satisfies

$$\int_{\Omega} \frac{\partial u}{\partial x_i} dV = \int_{\partial \Omega} u n_i dA,$$

where  $n_i$  is the ith component of the unit outward normal  $\mathbf{n}$  of  $\partial\Omega$ .

Apply Theorem 3 to uv and we have

**Lemma 2** (Integration-by-parts). For  $u, v \in C^1(\overline{\Omega})$ , we have

$$\int_{\Omega} \frac{\partial u}{\partial x_i} v \, dV = -\int_{\Omega} u \frac{\partial v}{\partial x_i} dV + \int_{\partial \Omega} u v n_i \, dA, \tag{34}$$

where  $n_i$  is the *i*th component of the unit outward normal  $\mathbf{n}$  of  $\partial\Omega$ . Replace v in (34) with  $\frac{\partial v}{\partial x_i}$ , sum over i, and we have

**Lemma 3** (Green's formula). For  $u, v \in C^2(\overline{\Omega})$ , we have

$$\int_{\Omega} \nabla u \cdot \nabla v \, dV = -\int_{\Omega} u \Delta v \, dV + \int_{\partial \Omega} u \frac{\partial v}{\partial \mathbf{n}} dA. \tag{35}$$

# 2.5 B-stable and algebraically stable RK methods

To solve an ODE system  $\mathbf{u}' = \mathbf{f}(\mathbf{u}, t)$ , an s-stage RK method is a one-step method of the form

$$\begin{cases} \mathbf{y}_i = \mathbf{f}(\mathbf{U}^n + k \sum_{j=1}^s a_{i,j} \mathbf{y}_j, t_n + c_i k), \\ \mathbf{U}^{n+1} = \mathbf{U}^n + k \sum_{j=1}^s b_j \mathbf{y}_j, \end{cases}$$
(36)

where i = 1, 2, ..., s and the coefficients  $a_{i,j}, b_j, c_i$  are real.

A function  $\mathbf{f}: \mathbb{R}^D \times [0, +\infty) \to \mathbb{R}^D$  satisfies a one-sided Lipschitz condition if

$$\forall t \ge 0, \forall \mathbf{u}, \mathbf{v} \in \mathbb{R}^{D}, \ \langle \mathbf{u} - \mathbf{v}, \ \mathbf{f}(\mathbf{u}, t) - \mathbf{f}(\mathbf{v}, t) \rangle \le \mu \|\mathbf{u} - \mathbf{v}\|^{2},$$
 (37)

where  $\mu$  is the one-sided Lipschitz constant of f. The ODE system is contractive or monotone if **f** satisfies (37) with  $\mu = 0$ .

A contractive ODE system is *dissipative*: for any solutions  $\mathbf{u}(t)$  and  $\mathbf{v}(t)$ , the norm  $\|\mathbf{u}(t) - \mathbf{v}(t)\|$  decreases monotonically as t increases. In other words, different solution trajectories of a contractive ODE system never depart from each other, and hence small perturbations remain small. For numerical methods, this leads to

**Definition 1** (B-stability [28]). A one-step method is B-stable if, for any contractive ODE system, every pair of its numerical solutions  $\mathbf{U}^n$  and  $\mathbf{V}^n$  satisfy

$$\forall n = 0, 1, \dots, \|\mathbf{U}^{n+1} - \mathbf{V}^{n+1}\| \le \|\mathbf{U}^n - \mathbf{V}^n\|.$$

It can be shown that B-stable methods are A-stable. **Definition 2.** An RK method is algebraically stable if

- 1. the RK weights  $b_1, b_2, \ldots, b_s$  are nonnegative,
- 2. the following symmetric matrix  $M \in \mathbb{R}^{s \times s}$  is positive semidefinite:

$$m_{i,j} = b_i a_{i,j} + b_j a_{j,i} - b_i b_j.$$
 (38)

An algebraically stable RK method is B-stable and thus A-stable [29].

# 3 The GePUP-E formulation

Boundary conditions of the evolutionary variable  $\mathbf{w}$  play a crucial role in establishing a stable numerical scheme. As elaborated in Subsection 1.2.4, the GePUP formulation (21) leads to the heat equation (22). However, neither the homogeneous Dirichlet nor the homogeneous Neumann condition is explicitly imposed on  $\nabla \cdot \mathbf{w}$  in (21), thus the dacay of  $\nabla \cdot \mathbf{w}$  is not guaranteed. To fix this glitch, we draw inspiration from the excellent work of Rosales, Shirokoff, and their colleagues [22, 23] to adapt "electric" boundary conditions into GePUP, proposing

**Definition 3.** The GePUP-E formulation of the INSE on no-slip domains is

$$\frac{\partial \mathbf{w}}{\partial t} = \mathbf{g} - \mathbf{u} \cdot \nabla \mathbf{u} - \nabla q + \nu \Delta \mathbf{w} \qquad in \ \Omega, \tag{39a}$$

$$\mathbf{w} \cdot \boldsymbol{\tau} = 0, \quad \nabla \cdot \mathbf{w} = 0 \qquad on \ \partial \Omega, \tag{39b}$$

$$\mathbf{u} = \mathscr{P}\mathbf{w} \qquad in \ \Omega, \tag{39c}$$

$$\mathbf{u} \cdot \mathbf{n} = 0 \qquad on \ \partial \Omega, \tag{39d}$$

$$\Delta q = \nabla \cdot (\mathbf{g} - \mathbf{u} \cdot \nabla \mathbf{u}) \qquad in \ \Omega, \tag{39e}$$

$$\mathbf{n} \cdot \nabla q = \mathbf{n} \cdot (\mathbf{g} - \mathbf{u} \cdot \nabla \mathbf{u} + \nu \Delta \mathbf{w}) + \lambda \mathbf{n} \cdot \mathbf{w} \quad on \ \partial \Omega, \tag{39f}$$

where  $\mathbf{u}$  is the divergence-free velocity in (1),  $\mathbf{w} = \mathbf{u} - \nabla \phi$  a non-solenoidal velocity for some scalar function  $\phi$ ,  $\mathbf{n}$  and  $\boldsymbol{\tau}$  the unit normal and unit tangent vector of  $\partial \Omega$ , respectively, and  $\lambda$  a nonnegative penalty parameter. The two velocities  $\mathbf{w}$  and  $\mathbf{u}$  have the same initial condition in  $\overline{\Omega}$ , the closure of  $\Omega$ , i.e.,

$$\forall \mathbf{x} \in \overline{\Omega}, \quad \mathbf{w}(\mathbf{x}, t_0) = \mathbf{u}(\mathbf{x}, t_0). \tag{40}$$

(39b) is different from (21b). First, the boundary condition  $\mathbf{n} \cdot \mathbf{w} = 0$  in (21b) is removed and the term  $\lambda \mathbf{n} \cdot \mathbf{w}$  is added in (39f) so that any nonzero  $\mathbf{n} \cdot \mathbf{w}$  decays exponentially towards zero; see Lemma 5. Second, the boundary condition  $\nabla \cdot \mathbf{w} = 0$  is added in (39b) to set up an exponential decay of  $\nabla \cdot \mathbf{w}$ ; see Theorem 4. Third, the boundary condition  $\mathbf{w} \cdot \boldsymbol{\tau} = 0$  is added in (39b) to close the vector diffusion equation governing the evolution of  $\mathbf{w}$ . Lastly, the boundary condition  $\mathbf{u} \cdot \boldsymbol{\tau} = 0$  in (21b) is removed because, as a perturbed version of  $\mathbf{u}$ , the non-solenoidal velocity  $\mathbf{w}$  is  $\mathbf{u}$  when the initial condition (40) is imposed; see Lemma 6. Another initial condition weaker than (40) is

$$\forall \mathbf{x} \in \partial \Omega, \quad \mathbf{w}(\mathbf{x}, t_0) = \mathbf{u}(\mathbf{x}, t_0). \tag{41}$$

To connect  $\mathbf{w}$  to  $\mathbf{u}$ , (39c) appears to be the most natural choice.

Compared to the formulation proposed in [22, 23], the GePUP-E formulation (39) facilitates the design and analysis of numerical schemes that treat the nonlinear convection term and the pressure gradient term explicitly; see Definition 6.

Lemma 4. The Neumann BVP (39c,d) admits a unique solution of u.

*Proof.* (39c,d) and the definition  $\mathbf{w} = \mathbf{u} - \nabla \phi$  yield

$$\Delta \phi = -\nabla \cdot \mathbf{w} \quad \text{in } \Omega, 
\mathbf{n} \cdot \nabla \phi = -\mathbf{n} \cdot \mathbf{w} \quad \text{on } \partial \Omega.$$
(42)

Then the proof is completed by Theorem 1 and the divergence theorem.

## 3.1 The exponential decay of $n \cdot w$ and $\nabla \cdot w$ in (39)

Although the no-penetration condition  $\mathbf{n} \cdot \mathbf{w} = 0$  is not explicitly stated in (39), the exponential decay of  $\mathbf{n} \cdot \mathbf{w}$  on  $\partial \Omega$  is guaranteed by

**Lemma 5.** The GePUP-E formulation (39) satisfies

$$\frac{\partial (\mathbf{n} \cdot \mathbf{w})}{\partial t} = -\lambda \mathbf{n} \cdot \mathbf{w} \quad on \ \partial \Omega$$
 (43)

and thus  $\mathbf{n} \cdot \mathbf{w}(t) = e^{-\lambda(t-t_0)} \mathbf{n} \cdot \mathbf{w}(t_0)$  holds on  $\partial \Omega$ . In particular, we have

$$\mathbf{n} \cdot \mathbf{w}(t_0) = 0 \implies \forall t > t_0, \ \mathbf{n} \cdot \mathbf{w}(t) = 0.$$

*Proof.* (43) follows immediately from (39f) and the normal component of (39a).  $\Box$ 

The exponential decay of  $\nabla \cdot \mathbf{w}$  is guaranteed by

**Theorem 4.** The GePUP-E formulation (39) satisfies

$$\frac{\partial \left(\nabla \cdot \mathbf{w}\right)}{\partial t} = \nu \Delta \left(\nabla \cdot \mathbf{w}\right) \quad in \ \Omega, \tag{44}$$

which implies

$$\frac{\mathrm{d}}{\mathrm{d}t} \|\nabla \cdot \mathbf{w}\|^2 = -2\nu \|\nabla (\nabla \cdot \mathbf{w})\|^2, \tag{45}$$

which further implies

$$\|\nabla \cdot \mathbf{w}(t)\| \le e^{-\nu C(t-t_0)} \|\nabla \cdot \mathbf{w}(t_0)\| \tag{46}$$

where  $t_0$  is the initial time and C a positive constant independent of  $\mathbf{w}$ .

*Proof.* (44) follows from the divergence of (39a), (39e), and the commutativity of  $\nabla$  and  $\Delta$ . Multiply (44) with  $\nabla \cdot \mathbf{w}$ , integrate over  $\Omega$ , and we have

$$\begin{split} & \frac{1}{2} \frac{\mathrm{d}}{\mathrm{d}t} \| \nabla \cdot \mathbf{w} \|^2 = \nu \left\langle \Delta \left( \nabla \cdot \mathbf{w} \right), \nabla \cdot \mathbf{w} \right\rangle \\ & = -\nu \left\| \nabla \left( \nabla \cdot \mathbf{w} \right) \right\|^2 + \nu \oint_{\partial \Omega} \left( \nabla \cdot \mathbf{w} \right) \frac{\partial \left( \nabla \cdot \mathbf{w} \right)}{\partial \mathbf{n}} \mathrm{d}A = -\nu \left\| \nabla \left( \nabla \cdot \mathbf{w} \right) \right\|^2, \end{split}$$

where the second step follows from Green's formula (35) with  $u = v = \nabla \cdot \mathbf{w}$  and the last from (39b). Then the Poincaré-Friedrichs inequality and (45) imply  $\frac{\mathrm{d}}{\mathrm{d}t} \|\nabla \cdot \mathbf{w}\|^2 \le -2\nu C \|\nabla \cdot \mathbf{w}\|^2$  and then (46) follows from

$$\frac{\mathrm{d}}{\mathrm{d}t} \left( e^{2\nu Ct} \|\nabla \cdot \mathbf{w}\|^2 \right) = e^{2\nu Ct} \left( 2\nu C \|\nabla \cdot \mathbf{w}\|^2 + \frac{\mathrm{d}}{\mathrm{d}t} \|\nabla \cdot \mathbf{w}\|^2 \right) \le 0.$$

Due to the exponential decay in (46), the convergence of  $\mathbf{w}$  to  $\mathbf{u}$  should be sufficiently fast for most practical applications. In numerical simulations via GePUP-E, it is suggested to set the initial condition of  $\mathbf{w}$  to that of  $\mathbf{u}$ . The mechanism of exponential decay in Theorem 4 is supposed to suppress divergence residue caused by truncation errors of spatial operators; see Theorem 5.

### 3.2 Recovering INSE from GePUP-E

**Lemma 6.** With the initial condition (40), the GePUP-E formulation (39) recovers the INSE (1) for all  $t \ge t_0$ .

*Proof.* (40) and (46) yield  $\nabla \cdot \mathbf{w}(t) = 0$ . With  $\mathbf{w} \cdot \mathbf{n} = 0$  in Lemma 5, the BVP (42) reduces to a Laplace equation with homogeneous Neumann conditions, for which  $\phi$  being a constant in  $\Omega$  is a particular solution. Thus  $\nabla \phi = \mathbf{0}$  and  $\mathbf{w} = \mathbf{u}$ .

Lemma 6 implies the well-posedness of (39e,f). In comparison to (21f), (39f) contains the convection term so that the well-posedness of the Neumann BVP (39e,f) is independent of the boundary condition of  $\mathbf{u}$ .

**Lemma 7.** With the initial condition (40), the Neumann BVP (39e,f) admits a unique solution of  $\nabla q$ .

*Proof.* The divergence theorem and the commutativity of  $\nabla$  and  $\Delta$  imply

$$\oint_{\partial\Omega} (\mathbf{n} \cdot \nu \Delta \mathbf{w} + \lambda \mathbf{n} \cdot \mathbf{w}) \, dA = \int_{\Omega} (\nu \Delta \nabla \cdot \mathbf{w} + \lambda \nabla \cdot \mathbf{w}) \, dV = 0,$$

where the second step follows from Lemma 6. The divergence theorem gives

$$\int_{\Omega} \nabla \cdot (\mathbf{g} - \mathbf{u} \cdot \nabla \mathbf{u}) \, dV = \oint_{\partial \Omega} \mathbf{n} \cdot (\mathbf{g} - \mathbf{u} \cdot \nabla \mathbf{u}) \, dA.$$

Then the rest of the proof follows from Theorem 1.

**Theorem 5.** GePUP-E (39) with the initial condition (41) satisfies

$$\forall \epsilon > 0, \ \exists t^* > t_0, \ s.t. \ \forall t > t^*, \quad \begin{cases} \sup_{\mathbf{x} \in \Omega} |\nabla \cdot \mathbf{w}(\mathbf{x}, t)| < \epsilon \\ \|\mathbf{w}(\mathbf{x}, t) - \mathbf{u}(\mathbf{x}, t)\| < \epsilon, \\ \|q(\mathbf{x}, t) - p(\mathbf{x}, t)\| < \epsilon. \end{cases}$$

*Proof.* The first limit follows from (46). The second limit then follows from arguments similar to those in the proof of Lemma 6. The third limit is a consequence of the second limit.

# 3.3 The equivalence of GePUP-E with INSE

To derive GePUP-E from INSE, we split  ${\bf u}$  into  $\nabla \phi$  and  ${\bf w}$  and suppress  $\nabla \cdot {\bf w}$  via a heat equation.

**Lemma 8.** The GePUP-E formulation (39) is derived from the INSE (1) by splitting the velocity  $\mathbf{u}$  as  $\mathbf{u} = \mathbf{w} + \nabla \phi$  and demanding that  $\mathbf{w}$  satisfy (39b) and (44).

*Proof.* For an arbitrary vector field  $\mathbf{u}$ , (20) and (28) yield

$$\Delta \mathcal{P}\mathbf{u} = \Delta(\mathbf{u} - \nabla \phi) = \Delta \mathbf{u} - \nabla \nabla \cdot \nabla \phi = \mathcal{B}\mathbf{u} + \nabla \nabla \cdot \mathcal{P}\mathbf{u},$$

and thus we have

$$\Delta \mathcal{P} = \Delta - \nabla \nabla \cdot + \nabla \nabla \cdot \mathcal{P}. \tag{47}$$

We deduce (39a) from

$$\frac{\partial \mathbf{w}}{\partial t} = \frac{\partial \mathcal{P} \mathbf{u}}{\partial t} = \mathcal{P} \frac{\partial \mathbf{u}}{\partial t} = \mathcal{P} \mathbf{a} - \nu (\Delta \mathbf{u} - \nabla \nabla \cdot \mathbf{u} + \nabla \nabla \cdot \mathcal{P} \mathbf{u} - \Delta \mathcal{P} \mathbf{u}) 
= \mathcal{P} \mathbf{a} - \mathbf{a}^* + \mathbf{g} - \mathbf{u} \cdot \nabla \mathbf{u} + \nu \nabla \nabla \cdot \mathbf{u} - \nu \nabla \nabla \cdot \mathbf{w} + \nu \Delta \mathbf{w} 
= \mathbf{g} - \mathbf{u} \cdot \nabla \mathbf{u} - \nabla q + \nu \Delta \mathbf{w},$$
(48)

where the third step follows from (47), the fourth from (12), and the last from

$$\nabla q := \mathbf{a}^* - \mathcal{P}\mathbf{a} - \nu\nabla\nabla \cdot \mathbf{u} + \nu\nabla\nabla \cdot \mathbf{w}; \tag{49}$$

the above RHS is indeed a gradient because of (20) and (11). (39e) follows from (44) and the divergence of (49), i.e.,

$$\Delta q = \nabla \cdot (\mathbf{g} - \mathbf{u} \cdot \nabla \mathbf{u}) - \left[ \frac{\partial \nabla \cdot \mathbf{w}}{\partial t} - \nu (\Delta \nabla \cdot \mathbf{w}) \right] \quad \text{in } \Omega.$$

(39f) follows from Lemma 5 and the normal components of (39a) on  $\partial\Omega$ , i.e.,

$$\mathbf{n} \cdot \nabla q = \mathbf{n} \cdot (\mathbf{g} - \mathbf{u} \cdot \nabla \mathbf{u} + \nu \Delta \mathbf{w}) + \frac{\partial (\mathbf{n} \cdot \mathbf{w})}{\partial t}.$$

An alternative interpretation of (48) might be illuminating. A given scalar field  $\phi$  furnishes a specific generic projection  $\mathcal{P}_{\phi}\mathbf{u} = \mathbf{u} - \nabla \phi$  that perturbs  $\mathbf{u}$  to be non-solenoidal. For any  $\phi$ , the composite operator  $\mathscr{P} \circ \mathcal{P}_{\phi}$  is the identity on the divergence-free vector space, i.e.,  $\nabla \cdot \mathbf{u} = 0$  implies  $\mathscr{P} \circ \mathcal{P}_{\phi} \mathbf{u} = \mathscr{P} \mathbf{w} = \mathbf{u}$  for any  $\mathcal{C}^1$  scalar field  $\phi$ . If the evolution of  $\mathbf{w} = \mathcal{P}_{\phi}\mathbf{u}$  in (48) did not have the exponential decay of  $\nabla \cdot \mathbf{w}$ , we would have to apply  $\mathscr{P}$  to  $\frac{\partial \mathbf{w}}{\partial t}$  to recover the INSE. However, the exponential decay of  $\nabla \cdot \mathbf{w}$  in Theorem 4 leads to the convergence of  $\mathbf{w}$  to  $\mathbf{u}$  in Lemma 5 and thus there is no need to recover  $\mathbf{u}$  from  $\mathbf{w}$ .

**Theorem 6.** GePUP-E in Definition 3 is equivalent to the INSE (1).

*Proof.* This follows directly from Lemma 6 and Lemma 8.

# 3.4 The monotonic decrease of the total kinetic energy

**Lemma 9.** A vector field  $\mathbf{v} \in \mathcal{C}^1(\Omega)$  with  $\nabla \cdot \mathbf{v} = 0$  in  $\Omega$  and  $\mathbf{v} \cdot \mathbf{n} = 0$  on  $\partial \Omega$  is orthogonal to the gradient field of any scalar function  $\phi \in \mathcal{C}^1(\Omega)$ , i.e.,

$$\langle \mathbf{v}, \nabla \phi \rangle = \int_{\Omega} \mathbf{v} \cdot \nabla \phi \, dV = 0.$$
 (50)

*Proof.* By the chain rule, we have

$$\int_{\Omega} \mathbf{v} \cdot \nabla \phi \, dV = \int_{\Omega} \nabla \cdot (\phi \mathbf{v}) dV - \int_{\Omega} \phi \nabla \cdot \mathbf{v} \, dV = \int_{\partial \Omega} \phi \mathbf{v} \cdot \mathbf{n} \, dA = 0,$$

where the second step follows from the divergence theorem and the divergence-free condition of  ${\bf v}$  and the last from the no-penetration boundary condition.

As a benefit of Lemma 9 to numerical methods, the accuracy of the computed velocity is largely decoupled from that of the pressure gradient; this orthogonality condition can be enforced to machine precision in the FV formulation.

**Definition 4.** The kinetic energy of a fluid with velocity **u** is

$$E_{kinetic} := \frac{1}{2} \|\mathbf{u}\|^2 = \frac{1}{2} \int_{\Omega} \mathbf{u} \cdot \mathbf{u} \, dV.$$
 (51)

**Theorem 7.** Suppose the body force  $\mathbf{g}$  in (39a) is conservative, i.e.,  $\mathbf{g} = -\nabla \varphi$  for some scalar field  $\varphi$  in  $\Omega$ . Then the evolution of the kinetic energy in the GePUP-E formulation in Definition 3 is governed by

$$\frac{\mathrm{d}}{\mathrm{d}t} E_{kinetic} = -\nu \|\nabla \mathbf{u}\|^2 := -\nu \sum_{i=1}^{D} \sum_{j=1}^{D} \int_{\Omega} \left| \frac{\partial u_i}{\partial x_j} \right|^2 \mathrm{d}V.$$

*Proof.* Without loss of generality, we may assume that  $\mathbf{g} = \mathbf{0}$  since  $\varphi$  can be absorbed into q. The inner product of  $\mathbf{u}$  and the momentum equation (39a) gives

(\*): 
$$\left\langle \frac{\partial \mathbf{w}}{\partial t}, \mathbf{u} \right\rangle = -\left\langle \mathbf{u} \cdot \nabla \mathbf{u}, \mathbf{u} \right\rangle - \left\langle \nabla q, \mathbf{u} \right\rangle + \left\langle \nu \Delta \mathbf{w}, \mathbf{u} \right\rangle.$$

The left-hand side (LHS) is computed as

$$\left\langle \frac{\partial \mathbf{w}}{\partial t}, \mathbf{u} \right\rangle = \left\langle \frac{\partial (\mathbf{u} - \nabla \phi)}{\partial t}, \mathbf{u} \right\rangle = \left\langle \frac{\partial \mathbf{u}}{\partial t}, \mathbf{u} \right\rangle - \left\langle \nabla \frac{\partial \phi}{\partial t}, \mathbf{u} \right\rangle = \left\langle \frac{\partial \mathbf{u}}{\partial t}, \mathbf{u} \right\rangle \\
= \frac{\mathrm{d}}{\mathrm{d}t} \left( \frac{1}{2} \int_{\Omega} \mathbf{u} \cdot \mathbf{u} \, \mathrm{d}V \right) = \frac{\mathrm{d}}{\mathrm{d}t} E_{\text{kinetic}}, \tag{52}$$

where the first step follows from the definition of  $\mathbf{w}$ , the second from the commutativity of  $\partial_t$  and  $\nabla$ , the third from (39c,d) and Lemma 9, and the last from (51).

The first RHS term in (\*) vanishes because

$$\langle \mathbf{u} \cdot \nabla \mathbf{u}, \mathbf{u} \rangle = \int_{\Omega} \mathbf{u} \cdot (\mathbf{u} \cdot \nabla \mathbf{u}) \, dV = \int_{\Omega} u_i \left( u_j \frac{\partial u_i}{\partial x_j} \right) dV = \frac{1}{2} \int_{\Omega} u_j \frac{\partial (u_i u_i)}{\partial x_j} dV$$

$$= -\frac{1}{2} \int_{\Omega} u_i u_i \frac{\partial u_j}{\partial x_j} dV + \frac{1}{2} \int_{\partial \Omega} u_i u_i u_j n_j \, dA$$

$$= -\frac{1}{2} \int_{\Omega} |\mathbf{u}|^2 (\nabla \cdot \mathbf{u}) \, dV + \frac{1}{2} \int_{\partial \Omega} |\mathbf{u}|^2 (\mathbf{u} \cdot \mathbf{n}) \, dA = 0,$$

where the fourth step, in Einstein summation convention, follows from Lemma 2. The second term in (\*) also vanishes because of Lemma 9. The third term is

$$\langle \Delta \mathbf{w}, \mathbf{u} \rangle = \langle \Delta (\mathbf{u} - \nabla \phi), \mathbf{u} \rangle = \langle \Delta \mathbf{u}, \mathbf{u} \rangle - \langle \nabla \Delta \phi, \mathbf{u} \rangle = \langle \Delta \mathbf{u}, \mathbf{u} \rangle$$
$$= \int_{\Omega} u_i \Delta u_i \, dV = -\int_{\Omega} \nabla u_i \cdot \nabla u_i \, dV + \int_{\partial \Omega} u_i \frac{\partial u_i}{\partial \mathbf{n}} \, dA = -\|\nabla \mathbf{u}\|^2,$$
(53)

where the first step follows from the definition of  $\mathbf{w}$ , the second from the commutativity of  $\Delta$  and  $\nabla$ , the third from (39c,d) and Lemma 9, the penultimate from Green's formula (35), and the last from the no-slip condition of  $\mathbf{u}$ , which holds from Lemma 6 and (39b,d).

#### 3.5 Prominent features of the GePUP-E formulation

GePUP-E is summarized as follows.

- 1. The sole evolutionary variable is the non-solenoidal velocity  $\mathbf{w}$ , with  $\mathbf{u}$  determined from  $\mathbf{w}$  via (39c,d) and q from  $\mathbf{u}$  and  $\mathbf{w}$  via (39e,f). This chain of determination  $\mathbf{w} \to \mathbf{u} \to q$  from Neumann BVPs is *instantaneous* and has nothing to do with time integration. Therefore, a time integrator in MOL can be employed in a black-box manner.
- 2. There is no ambiguity on which velocities should be projected and which should not in MOL; this resolves (RSN-1) discussed in Section 1.2.3.
- 3. Now that the main evolutionary variable  $\mathbf{w}$  in (39) is formally non-solenoidal, the Leray-Helmholtz projection  $\mathcal{P}$  only comes into the system (39) on the

RHS. Although still contributing to the local truncation error, the approximation error of a discrete projection to  $\mathcal{P}$  does not affect numerical stability of MOL; this resolves (RSN-2) in Section 1.2.3.

4. (39) comes with the built-in mechanisms of exponential decays of velocity divergence and total kinetic energy, which are conducive to the design of semi-discrete algorithms that ensure numerical stability and preserve physical structures of incompressible flows, c.f. Theorems 9 and 10.

# 4 The GePUP-ES formulation

The SAV approach, as introduced in [24, 25], has been proposed to develop time discretization schemes that are both efficient and stable for gradient flows. This approach was originally designed to create schemes that are linear, decoupled, unconditionally stable, and can achieve up to second-order accuracy. It has also been successfully extended to address the Navier-Stokes equations in [30–32].

More recently, based on the generalized SAV approach [33], Huang et al. have devised high-order consistent splitting schemes for the Navier-Stokes equations, with periodic boundary conditions in [34] and no-slip boundary conditions in [35].

In this section, we couple the GePUP-E formulation (39) to the SAV approach introduced in [24, 25] to deal with the nonlinear convection term  $\mathbf{u} \cdot \nabla \mathbf{u}$  so that unconditionally energy-stable numerical schemes can be constructed.

**Definition 5.** The GePUP-ES formulation of the INSE on no-slip domains is

$$\frac{\partial \mathbf{w}}{\partial t} = \mathbf{g} - r(t)\mathbf{u} \cdot \nabla \mathbf{u} - \nabla q + \nu \Delta \mathbf{w} \qquad in \Omega, \qquad (54a)$$

$$\mathbf{w} \cdot \boldsymbol{\tau} = 0, \quad \nabla \cdot \mathbf{w} = 0 \qquad on \partial\Omega, \qquad (54b)$$

$$\mathbf{w} \cdot \boldsymbol{\tau} = 0, \quad \nabla \cdot \mathbf{w} = 0 \qquad on \ \partial \Omega, \tag{54b}$$

$$\frac{\mathrm{d}r}{\mathrm{d}t} = I_{cv}(\mathbf{u}, \mathbf{u}),\tag{54c}$$

$$\mathbf{u} = \mathscr{P}\mathbf{w} \qquad in \ \Omega, \tag{54d}$$

$$\mathbf{u} \cdot \mathbf{n} = 0 \qquad on \ \partial \Omega, \tag{54e}$$

$$\Delta q = \nabla \cdot (\mathbf{g} - r(t)\mathbf{u} \cdot \nabla \mathbf{u}) \qquad in \ \Omega, \tag{54f}$$

$$\mathbf{n} \cdot \nabla q = \mathbf{n} \cdot (\mathbf{g} - r(t)\mathbf{u} \cdot \nabla \mathbf{u} + \nu \Delta \mathbf{w}) + \lambda \mathbf{n} \cdot \mathbf{w} \quad on \ \partial \Omega, \tag{54g}$$

where  $I_{cv}(\mathbf{u}, \mathbf{v}) := \int_{\Omega} (\mathbf{u} \cdot \nabla \mathbf{u}) \cdot \mathbf{v} \, dV$ , the SAV  $r(t) \equiv 1$ , and  $\lambda$  is a nonnegative penalty parameter.

The introduction of the SAV  $r(t) \equiv 1$  immediately implies  $\frac{dr}{dt} = 0$ . We can define the evolution of r(t) as the ODE in (54c) because, for no-slip conditions, we always have  $\langle \mathbf{u} \cdot \nabla \mathbf{u}, \mathbf{u} \rangle = 0$ . As a newly added evolutionary variable, the SAV r(t) is a doubleedged sword. On the one hand, it leads to a tighter coupling between **u** and **w**, which makes it difficult to orchestrate an implicit or semi-implicit RK method as solving a sequence of *linear* systems; see the discussions in Section 5.2. On the other hand, it preserves the monotonic decrease of the kinetic energy; see Theorems 8 and 10.

**Theorem 8.** Suppose that the body force g is conservative. Then the energy dissipation of the GePUP-ES formulation (54) is governed by

$$\frac{\mathrm{d}}{\mathrm{d}t} \left( E_{\text{kinetic}} + \frac{r^2}{2} \right) = -\nu \|\nabla \mathbf{u}\|^2.$$

*Proof.* Take inner product with  $\mathbf{u}$  in (54a), multiply (54c) by r(t), add up the resulting two equations, and we cancel the integral of the convection term to obtain  $\langle \frac{\partial \mathbf{w}}{\partial t}, \mathbf{u} \rangle + r(t)r'(t) = \langle \mathbf{g} - \nabla q + \nu \Delta \mathbf{w}, \mathbf{u} \rangle$ . The rest of the proof follows from (52), (53), and Lemma 9.

Theorem 4 also holds for GePUP-ES with exactly the same proof. Similarly, the GePUP-ES formulation (54) retains the advantage of GePUP-E that the temporal integration and spatial discretization are completely decoupled. Hence the fourth-order finite-volume discrete operators in [5] can be reused and we will focus on temporal integration hereafter.

# 5 Algorithms

Based on the GePUP-ES formulation, we construct numerical algorithms in this section to preserve the monotonic decrease of the modified kinetic energy, the divergence residue, and the magnitude of the normal velocity on the domain boundary.

#### 5.1 Semi-discrete GePUP-ES-RK schemes

These schemes follow directly from discretizing the GePUP-ES formulation (54) in time by the RK method (36).

**Definition 6.** A GePUP-ES-RK scheme for solving the INSE with no-slip conditions is a semidiscrete algorithm of the form

$$\begin{cases}
\mathbf{w}^{n+1} = \mathbf{w}^{n} + k \sum_{i=1}^{s} b_{i} \boldsymbol{\rho}^{(i)} & in \Omega, \\
r^{n+1} = r^{n} + k \sum_{i=1}^{s} b_{i} I_{cv}(\widetilde{\mathbf{u}}^{(i)}, \mathbf{u}^{(i)}), \\
\mathbf{u}^{n+1} = \mathscr{P} \mathbf{w}^{n+1} & in \Omega, \\
\mathbf{n} \cdot \mathbf{u}^{n+1} = 0 & on \partial\Omega,
\end{cases} (55)$$

where s is the number of stages of the employed RK method  $(A, \mathbf{b}, \mathbf{c})$ , the integral  $I_{cv}(\widetilde{\mathbf{u}}^{(i)}, \mathbf{u}^{(i)})$  is the same as that in Definition 5, the auxiliary velocity  $\widetilde{\mathbf{u}}^{(i)}$  is a suitable explicit approximation to  $\mathbf{u}(t^n + c_i k)$  and

$$\Delta q^{(i)} = \nabla \cdot \left( \mathbf{g}^{(i)} - r^{(i)} \widetilde{\mathbf{u}}^{(i)} \cdot \nabla \widetilde{\mathbf{u}}^{(i)} \right) \qquad in \ \Omega, \tag{56a}$$

$$\mathbf{n} \cdot \nabla q^{(i)} = \mathbf{n} \cdot \left( \mathbf{g}^{(i)} - r^{(i)} \widetilde{\mathbf{u}}^{(i)} \cdot \nabla \widetilde{\mathbf{u}}^{(i)} + \nu \Delta \mathbf{w}^{(i)} \right) + \lambda \mathbf{n} \cdot \mathbf{w}^{(i)} \quad on \ \partial \Omega,$$
 (56b)

$$\boldsymbol{\rho}^{(i)} := \mathbf{g}^{(i)} - r^{(i)} \widetilde{\mathbf{u}}^{(i)} \cdot \nabla \widetilde{\mathbf{u}}^{(i)} - \nabla q^{(i)} + \nu \Delta \mathbf{w}^{(i)}, \tag{56c}$$

$$\mathbf{w}^{(i)} = \mathbf{w}^n + k \sum_{j=1}^s a_{i,j} \boldsymbol{\rho}^{(j)} \qquad in \ \Omega, \tag{56d}$$

$$\mathbf{w}^{(i)} \cdot \boldsymbol{\tau} = 0, \ \nabla \cdot \mathbf{w}^{(i)} = 0 \qquad on \ \partial\Omega, \tag{56e}$$

$$r^{(i)} = r^n + k \sum_{j=1}^s a_{i,j} I_{cv}(\widetilde{\mathbf{u}}^{(j)}, \mathbf{u}^{(j)}),$$
(56f)

$$\mathbf{u}^{(i)} = \mathscr{P}\mathbf{w}^{(i)} \qquad in \ \Omega, \tag{56g}$$

$$\mathbf{n} \cdot \mathbf{u}^{(i)} = 0 \qquad on \ \partial \Omega. \tag{56h}$$

In Definition 6, the approximations  $\tilde{\mathbf{u}}^{(i)}$  in  $\Omega$  may be obtained by polynomial interpolation based on stage values of recent time steps. In this work, we fit a cubic polynomial  $\mathbf{p}$  from the known velocity  $\hat{\mathbf{u}}_n^{(j)}$  at time instances  $t^n + \hat{c}_j k$  with j = 0, 1, 2, 3 and then approximate  $\mathbf{u}(t^n + c_i k)$  with

$$\forall i = 1, \dots, s, \qquad \widetilde{\mathbf{u}}_n^{(i)} = \mathbf{p}\left(c_i k\right) := \sum_{j=0}^3 \hat{\mathbf{u}}_n^{(j)} \prod_{\ell \neq j} \frac{c_i - \hat{c}_\ell}{\hat{c}_j - \hat{c}_\ell}; \tag{57}$$

- 1. for the first two time steps n = 0, 1, we calculate  $\hat{\mathbf{u}}^{(j)}$  by GePUP-ERK [5], the explicit RK method for solving the GePUP formulation, with time step size  $\frac{1}{3}k$  and then fit  $\mathbf{p}$  in (57) with  $[\hat{c}_0, \hat{c}_1, \hat{c}_2, \hat{c}_3] = [0, \frac{1}{3}, \frac{2}{3}, 1]$ ;
- size  $\frac{1}{3}k$  and then fit **p** in (57) with  $[\hat{c}_0, \hat{c}_1, \hat{c}_2, \hat{c}_3] = [0, \frac{1}{3}, \frac{2}{3}, 1];$ 2. for  $n \geq 2$ , we first calculate  $\hat{\mathbf{u}}^{(3)} = \mathbf{u}^{n+1}$  by GePUP-ERK with time step size k and then fit **p** in (57) with  $[\hat{c}_0, \hat{c}_1, \hat{c}_2, \hat{c}_3] = [-2, -1, 0, 1].$

We emphasize that  $\hat{\mathbf{u}}_n^{(j)}$ ,  $\widetilde{\mathbf{u}}_n^{(i)}$ , and  $\mathbf{u}(t^n+c_ik)$  are all at the same location so that the interpolation is only in time; see Figure 1 for an illustration.

**Theorem 9.** Suppose the RK method employed in the GePUP-ES-RK scheme (56)–(55) is algebraically stable in the sense of Definition 2. Then (41) implies

$$\forall n \in \mathbb{N}, \quad \left\| \nabla \cdot \mathbf{w}^{n+1} \right\|^2 - \left\| \nabla \cdot \mathbf{w}^n \right\|^2 \le -2k\nu \sum_{i=1}^s b_i \left\| \nabla \left( \nabla \cdot \mathbf{w}^{(i)} \right) \right\|^2,$$
 (58)

$$\forall n \in \mathbb{N}, \ \forall \mathbf{x} \in \partial \Omega, \quad \left| \mathbf{n} \cdot \mathbf{w}^{n+1}(\mathbf{x}) \right|^2 - \left| \mathbf{n} \cdot \mathbf{w}^n(\mathbf{x}) \right|^2 \le -2k\lambda \sum_{i=1}^s b_i \left| \mathbf{n} \cdot \mathbf{w}^{(i)}(\mathbf{x}) \right|^2.$$
 (59)

$$\hat{\mathbf{u}}_{n}^{(0)} = \mathbf{u}^{n} \qquad \hat{\mathbf{u}}_{n}^{(1)} \qquad \hat{\mathbf{u}}_{n}^{(2)} \qquad \hat{\mathbf{u}}_{n}^{(3)}$$

$$t_{n} \qquad t_{n} + \frac{1}{3}k \qquad t_{n} + \frac{2}{3}k \qquad t_{n} + \frac{3}{3}k = t_{n+1}$$

$$\mathbf{u}^{n} \qquad \mathbf{\tilde{u}}_{n}^{(1)} \qquad \mathbf{\tilde{u}}_{n}^{(2)} \qquad \mathbf{\tilde{u}}_{n}^{(3)} \qquad \mathbf{u}^{n+1}$$

$$t_{n} \qquad t_{n} + c_{1}k \qquad t_{n} + c_{2}k \qquad t_{n} + c_{3}k \qquad t_{n+1}$$

$$(a) \quad (\text{EAU-1}) \text{ for } n = 0, 1$$

$$\hat{\mathbf{u}}_{n}^{(0)} = \mathbf{u}^{n-2} \qquad \hat{\mathbf{u}}_{n}^{(1)} = \mathbf{u}^{n-1} \qquad \hat{\mathbf{u}}_{n}^{(2)} = \mathbf{u}^{n} \qquad \hat{\mathbf{u}}_{n}^{(3)}$$

$$t_{n-2} \qquad t_{n-1} \qquad t_{n} \qquad t_{n+1} = t_{n} + k$$

$$\mathbf{u}^{n} \qquad \mathbf{\tilde{u}}_{n}^{(1)} \qquad \mathbf{\tilde{u}}_{n}^{(2)} \qquad \mathbf{\tilde{u}}_{n}^{(3)} \qquad \mathbf{u}^{n+1}$$

$$t_{n} \qquad t_{n} + c_{1}k \quad t_{n} + c_{2}k \quad t_{n} + c_{3}k \qquad t_{n+1}$$

$$(b) \quad (\text{EAU-2}) \text{ for } n \geq 2$$

**Fig. 1** Estimating  $\widetilde{\mathbf{u}}^{(i)}$  in GePUP-ES-RK by (57) and (EAU-1,2).

*Proof.* Take divergence of (56c), apply (56a) and the commutativity of  $\Delta$  and  $\nabla$ , and we have  $\nabla \cdot \boldsymbol{\rho}^{(i)} = \nu \Delta (\nabla \cdot \mathbf{w}^{(i)})$ . Then

$$\begin{split} & \left\langle \nabla \cdot \mathbf{w}^{n+1}, \nabla \cdot \mathbf{w}^{n+1} \right\rangle \\ &= \left\langle \nabla \cdot \mathbf{w}^{n} + k \sum_{i=1}^{s} b_{i} \nabla \cdot \boldsymbol{\rho}^{(i)}, \nabla \cdot \mathbf{w}^{n} + k \sum_{j=1}^{s} b_{j} \nabla \cdot \boldsymbol{\rho}^{(j)} \right\rangle \\ &= \left\langle \nabla \cdot \mathbf{w}^{n}, \nabla \cdot \mathbf{w}^{n} \right\rangle + k \sum_{i=1}^{s} b_{i} \left\langle \nabla \cdot \mathbf{w}^{n}, \nabla \cdot \boldsymbol{\rho}^{(i)} \right\rangle \\ &+ k \sum_{j=1}^{s} b_{j} \left\langle \nabla \cdot \mathbf{w}^{n}, \nabla \cdot \boldsymbol{\rho}^{(j)} \right\rangle + k^{2} \sum_{i=1}^{s} \sum_{j=1}^{s} b_{i} b_{j} \left\langle \nabla \cdot \boldsymbol{\rho}^{(i)}, \nabla \cdot \boldsymbol{\rho}^{(j)} \right\rangle \\ &= \left\langle \nabla \cdot \mathbf{w}^{n}, \nabla \cdot \mathbf{w}^{n} \right\rangle + k^{2} \sum_{i=1}^{s} \sum_{j=1}^{s} b_{i} b_{j} \left\langle \nabla \cdot \boldsymbol{\rho}^{(i)}, \nabla \cdot \boldsymbol{\rho}^{(j)} \right\rangle \\ &+ k \sum_{i=1}^{s} b_{i} \left\langle \nabla \cdot \mathbf{w}^{(i)} - k \sum_{j=1}^{s} a_{i,j} \nabla \cdot \boldsymbol{\rho}^{(j)}, \nabla \cdot \boldsymbol{\rho}^{(i)} \right\rangle \\ &+ k \sum_{j=1}^{s} b_{j} \left\langle \nabla \cdot \mathbf{w}^{(j)} - k \sum_{i=1}^{s} a_{j,i} \nabla \cdot \boldsymbol{\rho}^{(i)}, \nabla \cdot \boldsymbol{\rho}^{(j)} \right\rangle \\ &= \left\langle \nabla \cdot \mathbf{w}^{n}, \nabla \cdot \mathbf{w}^{n} \right\rangle - 2\nu k \sum_{i=1}^{s} b_{i} \left\| \nabla \left( \nabla \cdot \mathbf{w}^{(i)} \right) \right\|^{2} \\ &- k^{2} \sum_{i=1}^{s} \sum_{j=1}^{s} m_{i,j} \left\langle \nabla \cdot \boldsymbol{\rho}^{(i)}, \nabla \cdot \boldsymbol{\rho}^{(j)} \right\rangle, \end{split}$$

where the last step follows from (38), Green's formula (35), and (56e). By Definition 2, the algebraic stability implies the symmetric positive semi-definiteness of M and thus we have  $M = O\Lambda O^T$ , where O is an orthogonal matrix and  $\Lambda$  is a diagonal matrix with  $\lambda_{\ell} = \Lambda_{\ell,\ell} \geq 0$  for each  $\ell = 1, \ldots, s$ . Hence (58) follows from

$$\begin{split} & \sum_{i=1}^{s} \sum_{j=1}^{s} m_{i,j} \left\langle \nabla \cdot \boldsymbol{\rho}^{(i)}, \nabla \cdot \boldsymbol{\rho}^{(j)} \right\rangle \\ &= \sum_{i=1}^{s} \sum_{j=1}^{s} \left( \sum_{\ell=1}^{s} o_{i,\ell} \lambda_{\ell} o_{j,\ell} \right) \left\langle \nabla \cdot \boldsymbol{\rho}^{(i)}, \nabla \cdot \boldsymbol{\rho}^{(j)} \right\rangle \\ &= \sum_{\ell=1}^{s} \lambda_{\ell} \left\langle \sum_{i=1}^{s} o_{i,\ell} \nabla \cdot \boldsymbol{\rho}^{(i)}, \sum_{j=1}^{s} o_{j,\ell} \nabla \cdot \boldsymbol{\rho}^{(j)} \right\rangle \\ &= \sum_{\ell=1}^{s} \lambda_{\ell} \left\| \sum_{i=1}^{s} o_{i,\ell} \nabla \cdot \boldsymbol{\rho}^{(i)} \right\|^{2} \geq 0. \end{split}$$

(56b) and the normal component of (56c) imply  $\mathbf{n} \cdot \boldsymbol{\rho}^{(i)} = -\lambda \mathbf{n} \cdot \mathbf{w}^{(i)}$ . Then arguments similar to those for (58) yield (59).

Corollary 2. Suppose the RK method employed in the GePUP-ES-RK scheme (56)-(55) is algebraically stable in the sense of Definition 2. Then (40) implies

$$\forall n \in \mathbb{N}^+, \quad \begin{cases} \|\nabla \cdot \mathbf{w}^n\| = 0; \\ \forall i = 1, \dots, s, \quad \nabla \cdot \mathbf{w}^{(i)} = 0, \end{cases}$$
 (60)

$$\forall n \in \mathbb{N}^+, \quad \begin{cases} \|\nabla \cdot \mathbf{w}^n\| = 0; \\ \forall i = 1, \dots, s, \quad \nabla \cdot \mathbf{w}^{(i)} = 0, \end{cases}$$

$$\forall n \in \mathbb{N}^+, \quad \begin{cases} \mathbf{n} \cdot \mathbf{w}^n|_{\partial\Omega} = 0; \\ \forall i = 1, \dots, s, \quad \mathbf{n} \cdot \mathbf{w}^{(i)}|_{\partial\Omega} = 0. \end{cases}$$

$$(60)$$

*Proof.* The initial condition (40) states  $\nabla \cdot \mathbf{w}(t_0) = \nabla \cdot \mathbf{u}(t_0) = 0$  and  $\mathbf{n} \cdot \mathbf{w}(t_0)|_{\partial\Omega} = 0$  $\mathbf{n} \cdot \mathbf{u}(t_0)|_{\partial\Omega} = 0$ . Then the first clauses of (60) and (61) follow from Theorem 9 and (ABS-1) in Definition 2. (58) dictates  $\|\nabla(\nabla \cdot \mathbf{w}^{(i)})\| = 0$  for each stage. Then the second clause of (60) follows from the boundary condition  $\nabla \cdot \mathbf{w}|_{\partial\Omega} = 0$  in (39b). Similarly, (59) dictates the second clause of (61).

**Theorem 10.** Suppose that the body force **g** in the GePUP-E formulation is conservative, that the initial condition of  $\mathbf{w}$  is (40), and that the employed RK method in (56)-(55) is algebraically stable in the sense of Definition 2. Then the energy dissipation of the GePUP-ES-RK scheme (56)-(55) is governed by

$$\mathcal{E}\left(t^{n+1}\right) - \mathcal{E}(t^n) \le -k\nu \sum_{i=1}^s b_i \left\|\nabla \mathbf{u}^{(i)}\right\|^2,\tag{62}$$

where the modified energy is defined as  $\mathcal{E}(t^n) := \frac{1}{2} \left( \|\mathbf{u}^n\|^2 + |r^n|^2 \right)$ .

*Proof.* Denote  $\sigma^{(i)} := \mathscr{P} \rho^{(i)}$  and we have from (56c,d) and (55)

$$\forall i = 1, \dots, s, \quad \mathbf{u}^{(i)} = \mathscr{P}\mathbf{w}^{(i)} = \mathscr{P}\left(\mathbf{w}^n + k\sum_{j=1}^s a_{i,j}\boldsymbol{\rho}^{(j)}\right) = \mathbf{u}^n + k\sum_{j=1}^s a_{i,j}\boldsymbol{\sigma}^{(j)};$$
$$\mathbf{u}^{n+1} = \mathscr{P}\mathbf{w}^{n+1} = \mathscr{P}\left(\mathbf{w}^n + k\sum_{i=1}^s b_i\boldsymbol{\rho}^{(i)}\right) = \mathbf{u}^n + k\sum_{i=1}^s b_i\boldsymbol{\sigma}^{(i)}.$$

It follows that

$$\begin{split} \left\langle \mathbf{u}^{n+1}, \mathbf{u}^{n+1} \right\rangle &= \left\langle \mathbf{u}^n + k \sum_{i=1}^s b_i \boldsymbol{\sigma}^{(i)}, \mathbf{u}^n + k \sum_{j=1}^s b_j \boldsymbol{\sigma}^{(j)} \right\rangle \\ &= \left\langle \mathbf{u}^n, \mathbf{u}^n \right\rangle + k \sum_{i=1}^s b_i \left\langle \mathbf{u}^n, \boldsymbol{\sigma}^{(i)} \right\rangle + k \sum_{j=1}^s b_j \left\langle \mathbf{u}^n, \boldsymbol{\sigma}^{(j)} \right\rangle \\ &+ k^2 \sum_{i=1}^s \sum_{j=1}^s b_i b_j \left\langle \boldsymbol{\sigma}^{(i)}, \boldsymbol{\sigma}^{(j)} \right\rangle \\ &= \left\langle \mathbf{u}^n, \mathbf{u}^n \right\rangle + k \sum_{i=1}^s b_i \left\langle \mathbf{u}^{(i)} - k \sum_{j=1}^s a_{i,j} \boldsymbol{\sigma}^{(j)}, \boldsymbol{\sigma}^{(i)} \right\rangle \\ &+ k \sum_{j=1}^s b_j \left\langle \mathbf{u}^{(j)} - k \sum_{i=1}^s a_{j,i} \boldsymbol{\sigma}^{(i)}, \boldsymbol{\sigma}^{(j)} \right\rangle + k^2 \sum_{i=1}^s \sum_{j=1}^s b_i b_j \left\langle \boldsymbol{\sigma}^{(i)}, \boldsymbol{\sigma}^{(j)} \right\rangle \\ &= \left\langle \mathbf{u}^n, \mathbf{u}^n \right\rangle + 2k \sum_{i=1}^s b_i \left\langle \mathbf{u}^{(i)}, \boldsymbol{\sigma}^{(i)} \right\rangle - k^2 \sum_{i=1}^s \sum_{j=1}^s m_{i,j} \left\langle \boldsymbol{\sigma}^{(i)}, \boldsymbol{\sigma}^{(j)} \right\rangle \end{split}$$

where the last step follows from (38). Then (ABS-2) in Definition 2 yields

(\*): 
$$\langle \mathbf{u}^{n+1}, \mathbf{u}^{n+1} \rangle \leq \langle \mathbf{u}^n, \mathbf{u}^n \rangle + 2k \sum_{i=1}^s b_i \langle \mathbf{u}^{(i)}, \boldsymbol{\sigma}^{(i)} \rangle$$
.

Write  $\alpha_i := I_{cv}(\widetilde{\mathbf{u}}^{(i)}, \mathbf{u}^{(i)}) = \langle \widetilde{\mathbf{u}}^{(i)} \cdot \nabla \widetilde{\mathbf{u}}^{(i)}, \mathbf{u}^{(i)} \rangle$  for each stage  $i = 1, \ldots, s$ . Then

$$\begin{split} & \left\langle \boldsymbol{\sigma}^{(i)}, \mathbf{u}^{(i)} \right\rangle = \left\langle \mathscr{P} \boldsymbol{\rho}^{(i)}, \mathbf{u}^{(i)} \right\rangle = \left\langle \boldsymbol{\rho}^{(i)}, \mathbf{u}^{(i)} \right\rangle \\ & = \left\langle \mathbf{g}^{(i)} - \nabla q^{(i)}, \mathbf{u}^{(i)} \right\rangle - r^{(i)} \alpha_i + \nu \left\langle \Delta \mathbf{w}^{(i)}, \mathbf{u}^{(i)} \right\rangle = -r^{(i)} \alpha_i - \nu \left\| \nabla \mathbf{u}^{(i)} \right\|^2, \end{split}$$

where the first equality follows from  $\sigma^{(i)} = \mathcal{P} \rho^{(i)}$ , the second from (26), (56g,h), and Lemma 9, the third from (56c) and the definition of  $\alpha_i$ , and the last from **g** being conservative, Lemma 9, (53), and Corollary 2.

Since the Leray-Helmholtz projection has no control over the tangential velocity, in (56g) we would have  $\boldsymbol{\tau} \cdot \mathbf{u}^{(i)} \neq 0$  if  $\nabla \cdot \mathbf{w}^{(i)} \neq 0$ . Fortunately Corollary 2 dictates  $\nabla \cdot \mathbf{w}^{(i)} = 0$  and  $\mathbf{n} \cdot \mathbf{w}^{(i)}|_{\partial\Omega} = 0$ , then the Leray-Helmholtz projection in (56g) reduces to the identity. Thus the second integral in the last line of (53) vanishes in GePUP-ES-RK. A related observation is that, although  $\nabla q$  is orthogonal to  $\mathbf{w}$ , it cannot be arbitrary as it must make  $\boldsymbol{\rho}^{(j)}$  in (56d) divergence-free; otherwise the Leray-Helmholtz projection in (56g) would not reduce to the identity.

Substitute  $\langle \mathbf{u}^{(i)}, \boldsymbol{\sigma}^{(i)} \rangle = -r^{(i)}\alpha_i - \nu \|\nabla \mathbf{u}^{(i)}\|^2$  into (\*) and we have

$$\left\langle \mathbf{u}^{n+1}, \mathbf{u}^{n+1} \right\rangle \leq \left\langle \mathbf{u}^{n}, \mathbf{u}^{n} \right\rangle - 2k \sum_{i=1}^{s} b_{i} \alpha_{i} r^{(i)} - 2\nu k \sum_{i=1}^{s} b_{i} \left\| \nabla \mathbf{u}^{(i)} \right\|^{2}.$$

Similarly, the positive semi-definiteness of M in Definition 2 yields

$$\begin{split} & \left| r^{n+1} \right|^2 = \left( r^n + k \sum_{i=1}^s b_i \alpha_i \right)^2 \\ &= \left| r^n \right|^2 + k \sum_{i=1}^s b_i \alpha_i r^n + k \sum_{j=1}^s b_j \alpha_j r^n + k^2 \sum_{i=1}^s \sum_{j=1}^s b_i b_j \alpha_i \alpha_j \\ &= \left| r^n \right|^2 + k \sum_{i=1}^s b_i \alpha_i \left( r^{(i)} - k \sum_{j=1}^s a_{i,j} \alpha_j \right) \\ &+ k \sum_{j=1}^s b_j \alpha_j \left( r^{(j)} - k \sum_{i=1}^s a_{j,i} \alpha_i \right) + k^2 \sum_{i=1}^s \sum_{j=1}^s b_i b_j \alpha_i \alpha_j \\ &= \left| r^n \right|^2 + 2k \sum_{i=1}^s b_i \alpha_i r^{(i)} - k^2 \sum_{i=1}^s \sum_{j=1}^s m_{i,j} \alpha_i \alpha_j \\ &\leq \left| r^n \right|^2 + 2k \sum_{i=1}^s b_i \alpha_i r^{(i)}. \end{split}$$

The proof is completed by summing up the above two inequalities.

In the last step of the above proof, it is the auxiliary variable r in the GePUP-ES formulation that leads to the cancellation of  $2k\sum_{i=1}^{s}b_{i}\alpha_{i}r^{(i)}$ .

Except on staggered grids, the initial condition of  $\mathbf{w}$  being incompressible in (40) cannot be exactly fulfilled in practical computations. However, the mechanism of divergence decay ensures that  $\mathbf{w}$  converge to  $\mathbf{u}$  sufficiently fast; see Theorem 2. This is also related to the millennium problem on the well-posedness of the INSE. If the solution of the INSE blows up, then its divergence must blow up first. Therefore, our computation only works when the INSE admits a bounded solution. After all, one cannot expect to solve the millennium problem by reformulating INSE.

#### 5.2 Semi-implicit GePUP-ES-SDIRK schemes

In light of Theorems 9 and 10, one way to preserve the monotonic decrease of the kinetic energy and the exponential decay of the divergence residue is to employ an algebraically stable RK method in GePUP-ES-RK. Gauss-Legendre RK methods are

algebraically stable and have a minimal number of stages for a given temporal order of accuracy. However, their employment in GePUP-ES-RK necessitates either the coupling of all intermediate stage values of **w** or the use of complex arithmetic. Thus we turn to singly diagonal implicit RK (SDIRK) methods that satisfy

$$a_{i,j} = \begin{cases} 0 & \text{if } i < j; \\ \gamma \neq 0 & \text{if } i = j, \end{cases}$$
 (63)

aiming to design a family of GePUP-ES-SDIRK schemes that only consist of solving a sequence of linear BVPs with real arithmetic, one intermediate stage at a time. The core difficulty for this, as mentioned in Section 4, is the nonlinear tight coupling of  $\mathbf{u}$ ,  $\mathbf{w}$ , q and r. Our solution is

**Definition 7.** A GePUP-ES-SDIRK scheme is a GePUP-ES-RK scheme in which an algebraically stable SDIRK method is employed as the RK method and in which stage values for each intermediate stage i = 1, ..., s are decomposed as

$$\begin{cases}
\mathbf{w}^{(i)} = \mathbf{w}_{0}^{(i)} + \sum_{j=1}^{i} r^{(j)} \mathbf{w}_{j}^{(i)}, \\
\mathbf{u}^{(i)} = \mathbf{u}_{0}^{(i)} + \sum_{j=1}^{i} r^{(j)} \mathbf{u}_{j}^{(i)}, \\
q^{(i)} = q_{1}^{(i)} + r^{(i)} q_{2}^{(i)},
\end{cases} (64)$$

where  $\mathbf{w}_0^{(i)}, \mathbf{w}_1^{(i)}, \dots, \mathbf{w}_i^{(i)}, \ \mathbf{u}_0^{(i)}, \mathbf{u}_1^{(i)}, \dots, \mathbf{u}_i^{(i)}, \ and \ q_1^{(i)}, q_2^{(i)}$  are auxiliary variables for the ith stage, which consists of steps as follows,

1. solve for  $q_1^{(i)}$  from the Neumann BVP

$$\begin{cases} \Delta q_1^{(i)} = \nabla \cdot \mathbf{g}^{(i)} & \text{in } \Omega, \\ \mathbf{n} \cdot \nabla q_1^{(i)} = \mathbf{n} \cdot \left( \mathbf{g}^{(i)} + \nu \Delta \widetilde{\mathbf{w}}^{(i)} \right) + \lambda \mathbf{n} \cdot \widetilde{\mathbf{w}}^{(i)} & \text{on } \partial \Omega, \end{cases}$$

where  $\widetilde{\mathbf{w}}^{(i)}$  is an approximation of  $\mathbf{w}^{(i)}$  obtained by (57) and (EAU-1,2).

2. solve for  $q_2^{(i)}$  from the Neumann BVP

$$\begin{cases} \Delta q_2^{(i)} = -\nabla \cdot \left(\widetilde{\mathbf{u}}^{(i)} \cdot \nabla \widetilde{\mathbf{u}}^{(i)}\right) \ in \ \Omega, \\ \mathbf{n} \cdot \nabla q_2^{(i)} = -\mathbf{n} \cdot \left(\widetilde{\mathbf{u}}^{(i)} \cdot \nabla \widetilde{\mathbf{u}}^{(i)}\right) \ on \ \partial \Omega. \end{cases}$$

3. solve for  $\mathbf{w}_0^{(i)}$  and  $\mathbf{w}_\ell^{(i)}$  where  $\ell = 1, ..., i$  from BVPs with their boundary conditions in (56e).

$$\begin{cases} (1 - \nu \gamma k \Delta) \mathbf{w}_0^{(i)} = \mathbf{w}^n + k \sum_{j=1}^i a_{i,j} \left( \mathbf{g}^{(j)} - \nabla q_1^{(j)} \right) + \nu k \sum_{j=1}^{i-1} a_{i,j} \Delta \mathbf{w}_0^{(j)}; \\ (1 - \nu \gamma k \Delta) \mathbf{w}_\ell^{(i)} = -k a_{i,\ell} \left( \widetilde{\mathbf{u}}^{(\ell)} \cdot \nabla \widetilde{\mathbf{u}}^{(\ell)} + \nabla q_2^{(\ell)} \right) + \nu k \sum_{j=\ell}^{i-1} a_{i,j} \Delta \mathbf{w}_\ell^{(j)}. \end{cases}$$

4. compute  $\mathbf{u}_{\ell}^{(i)} = \mathscr{P}\mathbf{w}_{\ell}^{(i)}$  for  $\ell = 0, 1, \dots, i$ .

5. define  $\overline{\mathbf{u}}^{(i)} := \mathbf{u}_0^{(i)} + \sum_{\ell=1}^{i-1} r^{(\ell)} \mathbf{u}_{\ell}^{(i)}$  and calculate  $r^{(i)}$  by

$$\left(1 - \gamma k I_{cv}\left(\widetilde{\mathbf{u}}^{(i)}, \mathbf{u}_{i}^{(i)}\right)\right) r^{(i)} = r^{n} + \gamma k I_{cv}\left(\widetilde{\mathbf{u}}^{(i)}, \ \overline{\mathbf{u}}^{(i)}\right) + k \sum_{j=1}^{i-1} a_{i,j} I_{cv}\left(\widetilde{\mathbf{u}}^{(j)}, \ \mathbf{u}^{(j)}\right).$$

6. calculate  $\mathbf{w}^{(i)}$  and  $\mathbf{u}^{(i)}$  by (64).

The above steps (GES.1–6) are direct consequences of the GePUP-ES-RK scheme (56)–(55), the property (63) of SDIRK, and the decomposition (64).

Substitute the third decomposition in (64) into (56a,b), separate the terms with and without  $r^{(i)}$ , notice that  $r^{(i)}$  is a scalar, and we have (GES.1–2). In step (GES.1), we decouple  $q^{(i)}$  from  $\mathbf{w}^{(i)}$  by approximating  $\mathbf{w}^{(i)}$  with  $\widetilde{\mathbf{w}}^{(i)}$  using the same method for calculating  $\widetilde{\mathbf{u}}^{(i)}$ .

For SDIRK, the upper bound of the summation in (56d) is *i*. Substitute (64) into (56c,d), separate the terms with and without  $r^{(i)}$ , switch the summation order

$$\textstyle \sum_{j=1}^{i} a_{i,j} \sum_{\ell=1}^{j} r^{(\ell)} \Delta \mathbf{w}_{\ell}^{(j)} = \sum_{\ell=1}^{i} r^{(\ell)} \sum_{j=\ell}^{i} a_{i,j} \Delta \mathbf{w}_{\ell}^{(j)},$$

and we have (GES.3). Then (GES.4) follows from (56g).

(GES.5) follows from substituting the second decomposition in (64) into (56f),

$$r^{(i)} = r^n + \gamma k I_{cv} \left( \widetilde{\mathbf{u}}^{(i)}, \ \overline{\mathbf{u}}^{(i)} + r^{(i)} \mathbf{u}_i^{(i)} \right) + k \sum_{j=1}^{i-1} a_{i,j} I_{cv} \left( \widetilde{\mathbf{u}}^{(j)}, \ \mathbf{u}^{(j)} \right),$$

and moving the  $r^{(i)}$ -term on the RHS to the LHS. Finally, the parenthesis on the LHS of (GES.5) must be no less than 1 because of (53), Lemma 9, and the inner product of  $\mathbf{u}_{i}^{(i)}$  to the equation on  $\mathbf{w}_{i}^{(i)}$  in (GES.3).

(55) and (GES.1–6) are the complete algorithmic steps of GePUP-ES-SDIRK. Theorems 9 and 10 state that both the velocity divergence and the modified energy in GePUP-ES-SDIRK decrease monotonically provided that the employed SDIRK is algebraically stable; an example is given in (65).

In this work, we discretize the continuous spatial operators in Definition 7 by the fourth-order collocated finite-volume operators in [5, Sec. 3 & 4] to obtain a fully discrete GePUP-ES-SDIRK scheme. However, it is emphasized that what we have proposed is not a single scheme but a space of solvers, each of which can be easily constructed by making menu choices for 'orthogonal' policies that span the solver space. The orthogonal structure of this solver space is very conducive to reusing in a black-box manner the legacy of classical finite volume/difference methods and the wealth of theory and algorithms for numerically solving ODEs; see Table 1. It is the GePUP-E formulation that makes this black-box reuse possible.

It would be ideal if the conclusions of Theorems 9 and 10 could also hold in the fully discrete case. Unfortunately, for the finite volume discretization on collocated grids, the fully discrete counterparts of Theorems 9 and 10 only hold asymptotically, i.e., in the limit of k and h simultaneously approaching zero. We defer to future research the investigation of suitable spatial discretizations so that Theorems 9 and 10 also hold in the fully discrete case.

Table 1 Main orthogonal policies of fully discrete GePUP-ES-RKs.

Orthogonal policies	Our choice	Other possible options
time integration	the SDIRK method (65)	algebraically stable RK methods
temporal accuracy	the fourth order	the second, third, and fifth orders
spatial discretization	finite volume	finite difference
spatial accuracy	the fourth order	the second order
variable location	collocated (as in [5])	staggered
estimating $\widetilde{\mathbf{u}}^{(i)}$ and $\widetilde{\mathbf{w}}^{(i)}$		interpolate
in Definitions $6$ and $7$	(57) & (EAU-1,2)	both in time and in space

# 6 Tests

In this section, we test a particular fully discrete GePUP-ES-SDIRK scheme by several numerical experiments to confirm the analytic results in previous sections. We employ the fourth-order finite-volume discretizations in [5] and a fourth-order, algebraically stable SDIRK method proposed by Du, Ju & Lu [36],

Along with other possible options of the major orthogonal policies, we show in Table 1 our choices that constitute the particular GePUP-ES-SDIRK scheme to be tested. According to the analysis in Section 5, this particular INSE solver should be high-order accurate both in time and in space, preserve monotonic decrease of the total kinetic energy, and have an asymptotically vanishing velocity divergence.

In all tests, numerical implementations are performed on a rectangular domain in Cartesian coordinates and thus the electric boundary conditions in (39b) are enforced by setting homogeneous Dirichlet conditions for the tangential velocity components and a homogeneous Neumann condition for the normal velocity. The initial condition of cell-averaged velocity is calculated by Boole's rule, a sixth-order formula of Newton-Cotes quadrature. Since exact solutions are unavailable, we define the computational error via Richardson extrapolation, i.e., by the difference of the solution on the current grid and that of the next finer grid.

For different values of the penalty parameter  $\lambda = 1$ , 10, and 100, error norms resulting in all our numerical tests remain the same up to the first two significant digits; this differs from the results reported in [22, 23]. This is not surprising since projecting  $\mathbf{w}$  to  $\mathbf{u}$  with  $\mathbf{u} \cdot \mathbf{n} = 0$  in (39c,d) and setting  $\mathbf{w}^0 = \mathbf{u}^0$  in (40) already imply that  $|\mathbf{n} \cdot \mathbf{w}|$  be small. Nonetheless, a positive-valued  $\lambda$  guarantees the no-penetration condition be fulfilled. Hereafter in this section we only show results in the case of  $\lambda = 1$ .

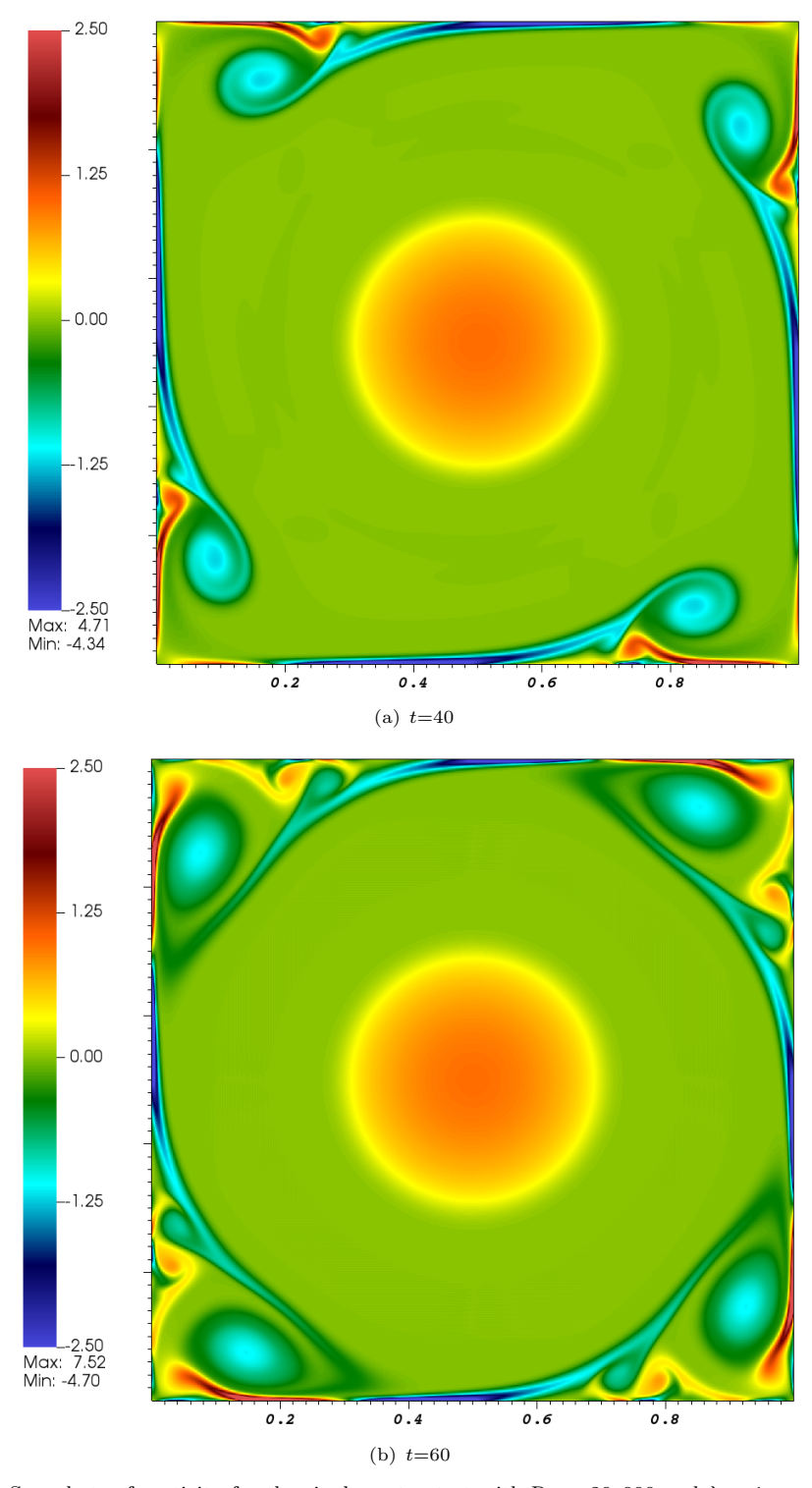


**Fig. 2** Snapshots of vorticity for the single-vortex test with Re = 20,000 and  $\lambda$  = 1 on a uniform grid with  $h = \frac{1}{1024}$ . The region of each cell is filled by a single color that corresponds to the cell-averaged vorticity. No image smoothing is applied.

**Table 2** Errors and convergence rates of GePUP-ES-SDIRK for the single-vortex test with Re = 20,000,  $t_0 = 0.0$ ,  $t_e = 60$ ,  $\lambda = 1$  and the Courant number Cr = 0.5.

h		$\frac{1}{256} - \frac{1}{512}$	Rate	$\frac{1}{512} - \frac{1}{1024}$	Rate	$\frac{1}{1024} - \frac{1}{2048}$
u	$L_{\infty}$	9.44e-04	3.63	7.61e-05	3.86	5.24e-06
	$L_1$	3.87e-05	3.76	2.86e-06	3.90	1.91e-07
	$L_2$	7.34e-05	3.73	5.52e-06	3.89	3.73e-07
$\nabla \cdot \mathbf{u}$	$L_{\infty}$	1.08e-02	2.03	2.64e-03	2.82	3.75e-04
	$L_1$	5.48e-05	3.38	5.27e-06	3.98	3.35e-07
	$L_2$	3.26e-04	2.47	5.87e-05	3.28	6.04e-06
q	$L_{\infty}$	8.96e-06	2.63	1.45e-06	2.94	1.89e-07
	$L_1$	7.91e-07	2.41	1.49e-07	2.50	2.63e-08
	$L_2$	1.38e-06	2.71	2.10e-07	2.59	3.50e-08
$\nabla q$	$L_{\infty}$	4.60e-04	2.58	7.67e-05	3.17	8.51e-06
	$L_1$	1.78e-05	3.28	1.83e-06	2.89	2.48e-07
	$L_2$	3.75 e-05	3.24	3.98e-06	3.00	4.96e-07

## 6.1 Single-vortex tests

Following [37], we define an axisymmetric velocity field on  $\Omega = [0, 1]^2$  by

$$u_{\theta}(r_{v}) = \begin{cases} \Gamma(\frac{1}{2}r_{v} - 4r_{v}^{3}) & \text{if } r_{v} < R; \\ \Gamma\frac{R}{r_{v}}(\frac{1}{2}R - 4R^{3}) & \text{if } r_{v} \ge R, \end{cases}$$
(66)

where  $r_v$  is the distance from the domain center  $(\frac{1}{2}, \frac{1}{2})^T$ . The choices R = 0.2 and  $\Gamma = 1$  give  $\max(u_\theta) = 0.068$ . A small viscosity  $\nu = 3.4 \times 10^{-6}$  yields a high Reynolds number Re = 20,000. The initial condition of velocity is obtained by projecting cell averages of **u** in (66) ten times to make it approximately divergence-free.

The tests are performed on four successively refined uniform grids. The time span [0,60] is made long enough for the turbulent boundary layers to develop prominent Lagrangian coherent structures. Snapshots of the vorticity at time t=40 and at the final time t=60 are shown in Figure 2, where the essential features of vortex sheet roll-up and counter-vortices agree with those in [37].

As shown in Table 2, the convergence rates of the velocity in all norms are close to 4. In contrast, convergence rates of the scalar q and its gradient have order reductions; this is due to the fact that the Neumann boundary condition in (54g) has to be obtained from spatial derivatives of the velocity and the calculation of these derivatives incurs order reductions in finite-volume discretizations.

Denote by  $\mathbf{U}_h^n$  and  $\mathbf{W}_h^n$  the finite-volume solutions that approximate cell averages of  $\mathbf{u}$  and  $\mathbf{w}$  at time  $t^n$ , respectively, and  $r_h^n$  the computed value of the SAV r at time  $t^n$ . The  $L_2$ -norm for a finite-volume solution  $\mathbf{V}_h^n$  is defined as  $\|\mathbf{V}_h^n\|_{\mathcal{C}}^2 := \sum_{\mathcal{C}_i} \|\mathcal{C}_i\| \cdot |\mathbf{V}_{h,i}^n|^2$  with  $\mathcal{C}_i$  ranging over all control volumes. The modified energy is then computed as  $\mathcal{E}_h^n := \frac{1}{2} \left( \|\mathbf{U}_h^n\|_{\mathcal{C}}^2 + |r_h^n|^2 \right)$ .

As shown in Figures 3(a,b),  $\mathcal{E}_h^n$  decreases monotonically over the entire simulation with  $|r_h^n - 1|$  remaining around  $10^{-11}$ , indicating that the (unmodified) kinetic energy  $\frac{1}{2} \|\mathbf{U}_h^n\|_{\mathcal{E}}^2$  also decreases monotonically.

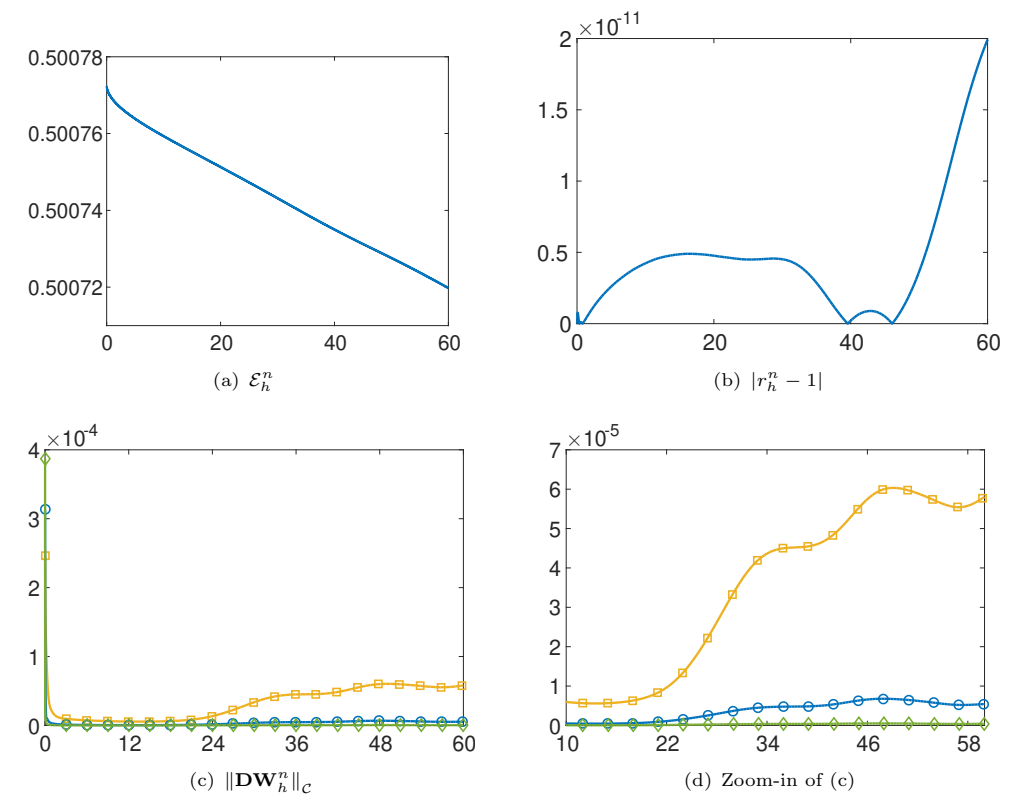


Fig. 3 Evolutions of the modified energy, the SAV, and velocity divergence in the single-vortex test with Re =  $2 \times 10^4$ , Cr = 0.5, and  $\lambda$  = 1. The abscissa in all subplots is time. In subplots (a) and (b),  $h = \frac{1}{1024}$ . In subplots (c) and (d), the curves marked by "square", "circle", and "diamond" represent the results for  $h = \frac{1}{512}$ ,  $\frac{1}{1024}$ , and  $\frac{1}{2048}$ , respectively.

In contrast, the  $L_2$ -norm of velocity divergence on the coarsest grid  $h = \frac{1}{512}$  shown in Figures 3(c,d) first decreases dramatically during the first several seconds, then gradually increases, and oscillates within a certain range. Furthermore, the range of oscillation decreases quickly as the grid is refined. To understand this evolution pattern, we consider the fully discrete counterpart of (58), i.e.,

$$\|\mathbf{DW}_{h}^{n+1}\|_{\mathcal{C}}^{2} - \|\mathbf{DW}_{h}^{n}\|_{\mathcal{C}}^{2} \le -2k\nu \sum_{i=1}^{s} b_{i} \|\mathbf{GDW}_{h}^{(i)}\|_{\mathcal{C}}^{2} + O(h^{p}),$$
 (67)

where **D** represents the discrete divergence, **G** the discrete gradient, and  $O(h^p)$  errors of spatial discretization. Our numerical results, such as those in Figure 3, suggest p > 1.

The key difference between (67) and (58) is the extra term  $O(h^p)$  in (67), which explains why the discrete divergence does not decay monotonically. Since the initial condition of  $\mathbf{w}(t_0)$  for this test is not divergence free, the RHS of (67) is dominated, in the early simulation stage, by the first term that contains  $\|\mathbf{GDW}_h^{(i)}\|_{\mathcal{C}}$ . Hence

**Table 3** Errors and convergence rates of GePUP-ES-SDIRK for the 2D viscous-box test with Re= $10^4$ ,  $t_0=0.0$ ,  $t_e=0.5$ , Cr = 0.5 and  $\lambda=1$ .

h	,	$\frac{1}{128} - \frac{1}{256}$	Rate	$\frac{1}{256} - \frac{1}{512}$	Rate	$\frac{1}{512} - \frac{1}{1024}$
	$L_{\infty}$	1.02e-03	3.20	1.10e-04	4.09	6.49e-06
u	$L_1$	4.10e-05	3.53	3.55e-06	3.94	2.32e-07
	$L_2$	9.85e-05	3.50	8.71e-06	3.96	5.59e-07
	$L_{\infty}$	7.33e-03	1.32	2.94e-03	2.44	5.41e-04
$ abla \cdot \mathbf{u}$	$L_1$	3.15e-04	3.18	3.47e-05	3.70	2.68e-06
	$L_2$	8.79e-04	2.22	1.89e-04	2.99	2.38e-05
q	$L_{\infty}$	4.17e-04	1.75	1.24e-04	1.96	3.18e-05
	$L_1$	6.61e-05	1.23	2.81e-05	1.70	8.69e-06
	$L_2$	9.92e-05	1.39	3.78e-05	1.73	1.14e-05
$\nabla q$	$L_{\infty}$	5.01e-03	1.70	1.54e-03	1.86	4.27e-04
	$L_1$	6.82e-04	1.71	2.08e-04	1.86	5.75e-05
	$L_2$	1.02e-03	1.69	3.15e-04	1.90	8.43e-05

(67) dictates the decay of the discrete divergence. However, as  $\|\mathbf{DW}_h^{(i)}\|_{\mathcal{C}}$  decreases continuously, the RHS of (67) eventually becomes dominated by  $O(h^p)$ . Then the inequality (67) loses control over the discrete divergence since  $O(h^p)$  is not negative-definite. When the discrete divergence increases to the degree such that the magnitude of  $O(h^p)$  is less than that of the other RHS term, the above pattern is repeated, leading to the oscillation of the discrete divergence. The bottom line is, however, that the discrete divergence is indirectly controlled by the term  $O(h^p)$  and thus the oscillation becomes less prominent as the grid is refined.

#### 6.2 Viscous-box tests

Following [9], we set the initial velocity on  $\Omega = [0, 1]^2$  to

$$\mathbf{u}(x,y) = \begin{pmatrix} \sin^2(\pi x) \sin(2\pi y) \\ -\sin(2\pi x) \sin^2(\pi y) \end{pmatrix}$$
 (68)

and advance cell-averaged initial values from  $t_0 = 0$  to  $t_e = 0.5$  on four successively refined uniform grids. Errors and convergence rates in the cases of Re =  $10^4$  and Re =  $10^2$  are shown in Tables 3 and 4, respectively.

For Re =  $10^4$ , convergence rates of the velocity in all norms are close to four. In contrast, those for Re =  $10^2$  are close to four in the  $L_1$ -norm and the  $L_2$ -norm, but are around 2.5 in the  $L_{\infty}$ -norm. Accordingly, convergence rates of  $\nabla q$  in the  $L_{\infty}$ -norm for Re =  $10^4$  are also substantially higher than those for Re =  $10^2$ .

These results are not out of expectations. We have proved in Theorem 5 that the pressure q converges to the pressure p and have shown in Section 2.3 that the pressure gradient  $\nabla p$  in the INSE can be split into two parts  $\nabla p = \nabla p_c + \nu \nabla p_s$ , where  $\nabla p_s$  responses to the Laplace-Leray commutator. When  $\nu$  is sufficiently large,  $\nu \nabla p_s$  dominates  $\nabla p_c$  and accounts for the bulk of  $\nabla p$ . Cozzi and Pego [38] showed that  $\|\nabla p_s\|$  may not be bounded at a boundary point that is not  $C^3$ . As a practical interpretation, the pressure could develop steep gradient at a  $C^1$  discontinuity of the domain boundary for low-Reynolds-number flows. Therefore, we believe that the order

**Table 4** Errors and convergence rates of GePUP-ES-SDIRK for the 2D viscous-box test with Re =  $10^2$ ,  $t_0 = 0.0$ ,  $t_e = 0.5$ , Cr = 0.1 and  $\lambda = 1$ 

h	,	$\frac{1}{64} - \frac{1}{128}$	Rate	$\frac{1}{128} - \frac{1}{256}$	Rate	$\frac{1}{256} - \frac{1}{512}$
	T	7.84e-06	2.46	1.43e-06	2.78	2.08e-07
	$L_{\infty}$					
u	$L_1$	2.03e-06	3.99	1.28e-07	4.04	7.76e-09
	$L_2$	2.63e-06	3.96	1.69e-07	3.99	1.07e-08
	$L_{\infty}$	3.90e-04	1.91	1.03e-04	2.02	2.55e-05
$ abla \cdot \mathbf{u}$	$L_1$	1.55e-05	3.83	1.09e-06	3.75	8.11e-08
	$L_2$	5.62e-05	3.24	5.96e-06	2.96	7.64e-07
	$L_{\infty}$	2.37e-04	1.83	6.67e-05	1.91	1.78e-05
q	$L_1$	3.33e-05	2.04	8.10e-06	2.05	1.95e-06
	$L_2$	5.09e-05	2.07	1.21e-05	2.06	2.92e-06
	$L_{\infty}$	4.92e-03	0.93	2.57e-03	0.42	1.92e-03
$\nabla q$	$L_1$	3.24e-04	1.97	8.26e-05	2.01	2.05e-05
	$L_2$	5.58e-04	1.72	1.69e-04	1.82	4.79e-05

reduction in the case of Re=10<sup>2</sup> is caused by the dominance of  $\nu\nabla p_s$  and the sharp corners ( $C^1$  discontinuities) of the square domain.

As shown in Figures 4(a,b), the modified energy  $\mathcal{E}_h^n$  decreases monotonically over the entire simulation for both Re =  $10^4$  and Re =  $10^2$ . It is also clear that the modified energy decreases faster in the higher-viscosity case. This confirms Theorem 10. Figures 4(c,d) show that the deviation of SAV from 1 is at most  $10^{-10}$ , thus the (unmodified) kinetic energy also decreases monotonically.

For both Re =  $10^4$  and Re =  $10^2$ , the evolution of the  $L_2$ -norm of velocity divergence shown in Figures 4(e,f) has essentially the same pattern: the  $L_2$ -norm first increases to a local maximum and then decreases. This pattern is different from that shown in Figures 3(c,d), but can still be very well explained by (67). Since the initial velocity (68) is perfectly divergence-free, the magnitude of  $\|\mathbf{GDW}_h^{(i)}\|_{\mathcal{C}}$  is small in the early simulation stage, during which the inequality (67) has no control over the discrete velocity divergence yet. However, as the discrete divergence accumulates to the point when the RHS of (67) gets dominated by its first term, the inequality (67) takes effect and forces the discrete divergence to decrease.

## 7 Conclusions

We have shown that the INSE with no-slip conditions can be equivalently reformulated as variants of the GePUP formulation [5], where the main evolutionary variable is a non-solenoidal velocity with electric boundary conditions whose divergence, controlled by a heat equation with homogeneous Dirichlet boundary conditions, decays exponentially. This GePUP-E reformulation is suitable for numerically solving the INSE because

- time integration and spatial discretization are completely decoupled so that highorder INSE solvers can be easily obtained from menu choices of orthogonal policies,
- the constituting modules such as a time integrator are employed in a black-box manner so that no internal details of any module are needed in building the INSE solver,

- the influences of nonzero velocity divergence upon numerical stability and accuracy are clear,
- a coupling of GePUP-E to SAV yields semi-discrete schemes with monotonically decreasing kinetic energy.

Results of numerical experiments confirm the analysis.

The next step along this line of research is to improve our current spatial discretizations so that fully discrete algorithms that ensure decays of velocity divergence and total kinetic energy can be constructed. Additionally, we are considering other types of boundary conditions such as the nonhomogeneous Dirichlet conditions, the radiation conditions, and mixed conditions. Also, we are currently augmenting the GePUP-ES solver to adaptive mesh refinement and parallel computing for an enhanced resolution of the multiple time scales and length scales in flows at moderate or high Reynolds numbers. Another work in progress is the development of GePUP solvers for the INSE with moving boundaries.

# Acknowledgments

The authors thank Prof. Buyang Li from the Hong Kong Polytechnic University for helpful discussions.

## References

- [1] Fefferman, C.L.: Existence and smoothness of the Navier-Stokes equation. In: The Millennium Prize Problems, pp. 57–67. Clay Math. Inst., Cambridge (2006)
- [2] Smale, S.: Mathematical problems for the next century. Math. Intell. **20**(2), 7–15 (1998)
- [3] Devlin, K.: The Millennium Problems: The Seven Greatest Unsolved Mathematical Puzzles of Our Time. New York, Basic Books (2003)
- [4] Li, B.: A bounded numerical solution with a small mesh size implies existence of a smooth solution to the Navier-Stokes equations. Numer. Math. 147(2), 283–304 (2021)
- [5] Zhang, Q.: GePUP: Generic projection and unconstrained PPE for fourth-order solutions of the incompressible Navier-Stokes equations with no-slip boundary conditions. J. Sci. Comput. 67(3), 1134–1180 (2016)
- [6] Chorin, A.J.: Numerical solution of the Navier-Stokes equations. Math. Comput. 22(104), 745-762 (1968)
- [7] Temam, R.: Sur l'approximation de la solution des équations de Navier-Stokes par la méthode des pas fractionnaires II. Arch. Ration. Mech. Anal. **33**, 377–385 (1969)

- [8] Kim, J., Moin, P.: Application of a fractional-step method to incompressible Navier-Stokes equations. J. Comput. Phys. **59**(2), 308–323 (1985)
- [9] Bell, J.B., Colella, P., Glaz, H.M.: A second-order projection method for the incompressible Navier-Stokes equations. J. Comput. Phys. 85(2), 257–283 (1989)
- [10] Orszag, S.A., Israeli, M., Deville, M.O.: Boundary conditions for incompressible flows. J. Sci. Comput. 1(1), 75–111 (1986)
- [11] E, W., Liu, J.-G.: Gauge method for viscous incompressible flows. Comm. Math. Sci. 1(2), 317–332 (2003)
- [12] Guermond, J.L., Minev, P., Shen, J.: An overview of projection methods for incompressible flows. Comput. Methods Appl. Mech. Engrg. 195(44-47), 6011– 6045 (2006)
- [13] Brown, D.L., Cortez, R., Minion, M.L.: Accurate projection methods for the incompressible Navier-Stokes equations. J. Comput. Phys. 168(2), 464–499 (2001)
- [14] Benzi, M., Golub, G.H., Liesen, J.: Numerical solution of saddle point problems. Acta Numer. 14, 1–137 (2005)
- [15] Gresho, P.M., Sani, R.L.: On pressure boundary conditions for the incompressible Navier-Stokes equations. Int. J. Numer. Methods Fluids **7**(10), 1111–1145 (1987)
- [16] Sanderse, B., Koren, B.: Accuracy analysis of explicit Runge-Kutta methods applied to the incompressible Navier-Stokes equations. J. Comput. Phys. 231(8), 3041–3063 (2012)
- [17] Kleiser, L., Schumann, U.: Treatment of incompressibility and boundary conditions in 3-D numerical spectral simulations of plane channel flows. In: Proceedings of the Third GAMM Conference on Numerical Methods in Fluid Mechanics. Notes on Numerical Fluid Mechanics, vol. 2, pp. 165–173. Springer, Berlin (1980)
- [18] Henshaw, W.D.: A fourth-order accurate method for the incompressible Navier-Stokes equations on overlapping grids. J. Comput. Phys. **113**(1), 13–25 (1994)
- [19] Johnston, H., Liu, J.-G.: Accurate, stable and efficient Navier-Stokes solvers based on explicit treatment of the pressure term. J. Comput. Phys. 199(1), 221–259 (2004)
- [20] Liu, J.-G., Liu, J., Pego, R.L.: Stability and convergence of efficient Navier-Stokes solvers via a commutator estimate. Comm. Pure Appl. Math. 60(10), 1443–1487 (2007)
- [21] Liu, J.-G., Liu, J., Pego, R.L.: Stable and accurate pressure approximation for unsteady incompressible viscous flow. J. Comput. Phys. **229**(9), 3428–3453

(2010)

- [22] Shirokoff, D., Rosales, R.R.: An efficient method for the incompressible Navier-Stokes equations on irregular domains with no-slip boundary conditions, high order up to the boundary. J. Comput. Phys. **230**(23), 8619–8646 (2011)
- [23] Rosales, R.R., Seibold, B., Shirokoff, D., Zhou, D.: High-order finite element methods for a pressure poisson equation reformulation of the Navier-Stokes equations with electric boundary conditions. Comput. Methods Appl. Mech. Engrg. 373, 113451 (2021)
- [24] Shen, J., Xu, J., Yang, J.: The scalar auxiliary variable (SAV) approach for gradient flows. J. Comput. Phys. **353**, 407–416 (2018)
- [25] Shen, J., Xu, J., Yang, J.: A new class of efficient and robust energy stable schemes for gradient flows. SIAM Rev. **61**(3), 474–506 (2019)
- [26] Taylor, M.E.: Partial Differential Equations I, 2nd edn. Applied Mathematical Sciences, vol. 115, pp. 408–409. Springer, Berlin (2011)
- [27] Munkres, J.: Analysis on Manifolds. CRC Press, Boca Raton (1997)
- [28] Butcher, J.C.: A stability property of implicit Runge-Kutta methods. BIT 15, 358–361 (1975)
- [29] Hairer, E., Wanner, G.: Solving Ordinary Differential Equations II: Stiff and Differential-Algebraic Problems, 2nd edn. Springer, Berlin (1996)
- [30] Li, X., Shen, J., Liu, Z.: New SAV-pressure correction methods for the Navier-Stokes equations: stability and error analysis. Math. Comput. 91(333), 141–167 (2022)
- [31] Lin, L., Yang, Z., Dong, S.: Numerical approximation of incompressible Navier-Stokes equations based on an auxiliary energy variable. J. Comput. Phys. 388, 1-22 (2019)
- [32] Li, X., Shen, J.: Error analysis of the SAV-MAC scheme for the Navier-Stokes equations. SIAM J. Numer. Anal. **58**(5), 2465–2491 (2020)
- [33] Huang, F., Shen, J.: A new class of implicit-explicit BDFk SAV schemes for general dissipative systems and their error analysis. Comput. Methods Appl. Mech. Engrg. **392**, 114718 (2022)
- [34] Huang, F., Shen, J.: Stability and error analysis of a class of high-order IMEX schemes for Navier-Stokes equations with periodic boundary conditions. SIAM J. Numer. Anal. **59**, 2926–2954 (2021)
- [35] Wu, K., Huang, F., Shen, J.: A new class of higher-order decoupled schemes for the

- incompressible Navier-Stokes equations and applications to rotating dynamics. J. Comput. Phys.  $\bf 458$ , 111097 (2022)
- [36] Du, Q., Ju, L., Lu, J.: Analysis of fully discrete approximations for dissipative systems and application to time-dependent nonlocal diffusion problems. J. Sci. Comput. **78**(3), 1438–1466 (2019)
- [37] Bell, J.B., Colella, P., Howell, L.H.: An efficient second order projection method for viscous incompressible flow. In: AIAA 10th Comp. Fluid Dynamics Conf., pp. 360–367 (1991)
- [38] Cozzi, E., Pego, R.L.: On optimal estimates for the Laplace-Leray commutator in planar domains with corners. Proc. Amer. Math. Soc. **139**(5), 1691–1706 (2011)

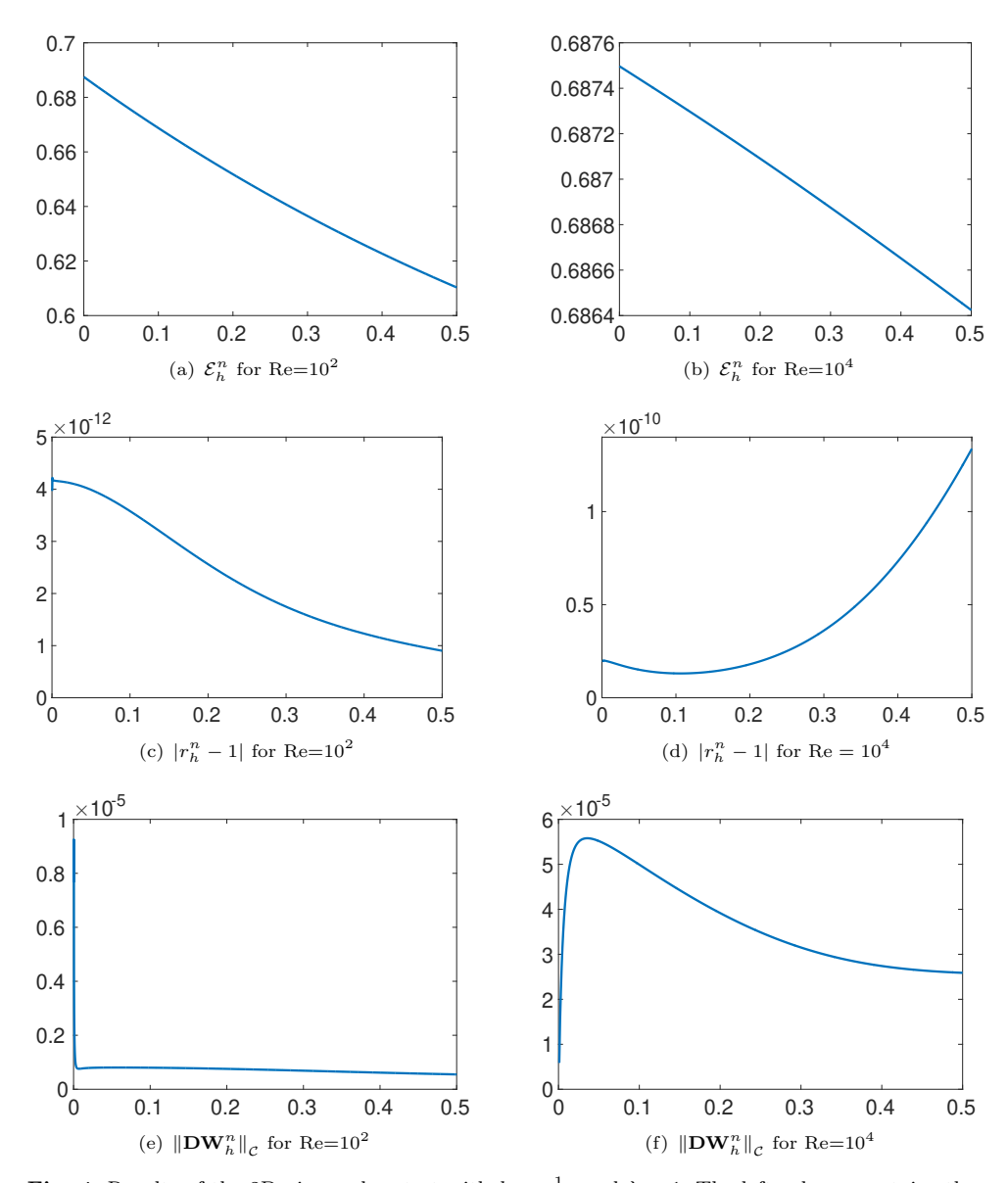


Fig. 4 Results of the 2D viscous-box test with  $h=\frac{1}{512}$  and  $\lambda=1$ . The left column contains those with Re = 100 and Cr = 0.1 while the right column those with Re =  $10^4$  and Cr = 0.5. The abscissa in all subplots is time.